Atmospheric Frontogenesis Models: Mathematical Formulation and Solution

BRIAN J. HOSKINS
National Center for Atmospheric Research,[1] *Boulder, Colo. 80302*

AND FRANCIS P. BRETHERTON
Dept. of Earth and Planetary Sciences, The Johns Hopkins University, Baltimore, Md. 21218

(Manuscript received 11 May 1971, in revised form 1 October 1971)

ABSTRACT

The approximation of geostrophic balance across a front is studied. Making this approximation, an analytic approach is made to a frontogenesis model based on the classic horizontal deformation field. Kelvin's circulation theorem suggests the introduction of a new independent variable in the cross-front direction. The problem is solved exactly for a Boussinesq, uniform potential vorticity fluid. Non-Boussinesq, non-uniform potential vorticity, latent heat, and surface friction effects are all studied. Using a two-region fluid we model the effects of confluence near the tropopause. A similar approach is made to the appearance of fronts in the finite-amplitude development of the simplest Eady wave; this is also solved analytically. Based on the surface fronts produced by these models, we give a general model of a strong surface front. There is a tendency to form discontinuities in a finite time.

1. Introduction

There are at least eight mechanisms which may be important in changing temperature gradients and forming atmospheric fronts (Fig. 1): (i) a horizontal deformation field, stretching in one horizontal dimension balanced by contraction in another, (ii) a horizontal shearing motion, (iii) a vertical deformation field, stretching or contraction in one horizontal dimension balanced by vertical displacements, (iv) differential vertical motion, (v) latent heat release, (vi) surface friction, (vii) turbulence and mixing, and (viii) radiation.

A horizontal deformation field is the classical frontogenetic mechanism postulated by Bergeron (1928). In Fig. 2, which is a schematic representation of a nascent extratropical cyclone, there is clearly horizontal stretching at A along the isotherms and contraction across them. The instantaneous circulation in vertical planes induced by a horizontal deformation field acting on a given temperature distribution has been investigated by Sawyer (1956), and the subsequent time development by Stone (1966), Williams and Plotkin (1968) and Williams (1968) using quasi-geostrophic theory. Such circulations formed large gradients in temperature at the ground, but discontinuities did not occur in a finite time. Their "fronts" were vertical and had large negative, as well as positive, relative vorticity. The reason that their results are not realistic is that the quasi-geostrophic equations are not valid as soon as gradients in temperature and wind velocity become com-

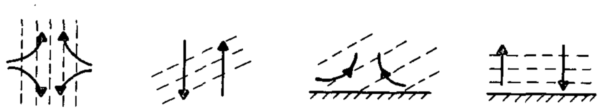

FIG. 1. Four mechanisms for changing horizontal temperature gradients: (i) horizontal deformation, (ii) horizontal shear, (iii) vertical deformation, (iv) differential vertical motion.

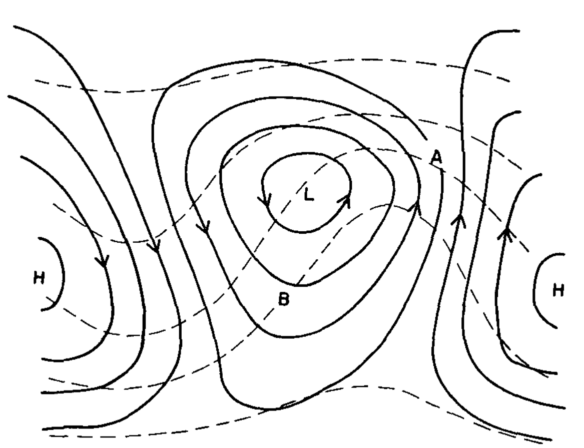

FIG. 2. Schematic extratropical cyclone (L) and anticyclone (H). Continuous lines represent isobars and broken lines isotherms. Large-scale flow is around the isobars in the direction shown. The temperature gradient at A is changed by horizontal deformation and that at B by horizontal shear.

[1] The National Center for Atmospheric Research is sponsored by the National Science Foundation.

parable with those observed in the weakest atmospheric fronts.

The horizontal shear mechanism (ii) is obviously important at B. There are cold northerly winds to the west and warm southerly winds to the east, which, if they persist, will lead to a large horizontal temperature contrast. Observation indicates that this effect is crucial at many cold fronts. Williams (1967) performed numerical integrations on a model in which it was dominant initially. He found that a realistic cold front formed.

The vertical deformation field (iii) is crucial in the dynamics of frontal systems. Sawyer (1956) and Eliassen (1962) have studied this field associated with particular geostrophic velocity and temperature distributions similar to those observed in frontal regions. These were primarily diagnostic studies, and the development with time was not considered.

Differential vertical motion (iv) can have either frontolytic or frontogenetic effects. It has been found to be largely responsible for the lack of sharpness of surface fronts in the middle troposphere (Sanders, 1955). On the other hand, temperature gradients in upper tropospheric fronts are intensified by the associated upgliding and subsidence (Reed, 1955).

In this paper we distinguish between large-scale geostrophic processes which intensify horizontal temperature gradients, and smaller scale ageostrophic motions embedded in the baroclinic flow which lead to the rapid formation of a near discontinuity. Mechanisms (i) and (ii) operate on the synoptic quasi-geostrophic scale, whereas (iii) and (iv) are dominant on the frontal scale and are not directly associated with large-scale weather systems. By considering situations in which intensification is occurring, we show how the ageostrophic effects and true front formation arise as a response to the increasing temperature gradient.

Numerical work by Arakawa (1962), Edelmann (1963) and others has shown that various forms of the equations of motion of a fluid on a rotating earth are capable of producing large gradients in physical quantities similar to those occurring in atmospheric fronts. Edelmann used a five-layer model of a fluid between two lateral boundaries. The basic state was a linear zonal thermal wind from the west increasing from zero at the surface to a maximum at 300 mb in the middle of the channel. On this he imposed a small-amplitude wave disturbance. As this disturbance grew into a strong cyclone-anticyclone system, sharp fronts formed. This happened despite horizontal and vertical diffusion of heat and momentum, with and without surface friction, and with no latent heat release. The experimental work of Fultz (1952) and Faller (1956) has shown that fronts can be reproduced in laboratory experiments using differentially heated rotating water. Therefore, we can conclude that we may use the "primitive" equations for our study, and that latent heat (v) and surface friction (vi), although important in the detailed formation of each front, are not essential for the frontogenetic process.

Mixing processes (vii) can smooth temperatures in one region, thus creating sharper temperature gradients at the edge of this region. Equally, the smoothing will lessen the gradients in the region concerned. We consider that mixing is not a basic mechanism of frontogenesis but that it provides the frontolytic effect which, when gradients are extremely large, eventually balances other frontogenetic processes.

Radiation (viii) is not important on the time and length scales of frontogenesis.

In this paper we exhibit a new mathematical approach to two of the simplest models exhibiting effects (i) and (ii) directly, but also implying (iii) and (iv). The basic approximation made is that in the direction of strongest gradients there is geostrophic balance, i.e., balance between pressure and Coriolis forces. Large-scale extratropical atmospheric flow is always approximately geostrophic. Geostrophic balance across a front is an approximation which observation suggests is quite accurate. Long-front (horizontal direction tangential to the front) accelerations are, however, important. The consistency of any solution found using this balance may be checked by comparing the neglected cross-front acceleration with the Coriolis and pressure forces. The approximations underlying the quasi-geostrophic theory (Pedlosky, 1964) are, however, much more restrictive and are certainly not valid in a true frontal situation. The variation of the Coriolis parameter (twice the vertical component of the earth's rotation) with latitude is also neglected since on the length scales characteristic of fronts it has little effect.

In an inviscid, adiabatic system potential vorticity is conserved. It is shown, provided this quantity is sufficiently smoothly distributed, that discontinuities in velocity and temperature can occur only at a boundary. This suggests that we should look for frontogenesis either at the surface (cf. surface fronts) or at discontinuities in potential vorticity (cf. upper tropospheric fronts).

We consider two rather different situations, and approach both using the primitive equations for an inviscid, adiabatic fluid, but concentrating on a Lagrangian viewpoint following fluid particles.

In the first situation we have a horizontally unbounded fluid between two surfaces. An initial temperature distribution independent of one horizontal coordinate is acted upon by a horizontal deformation field independent of height and with axis of contraction perpendicular to lines of constant temperature (mechanism 2). We discuss a hierarchy of models. In the simplest (Section 3c), the potential vorticity is zero everywhere. Although this is unrepresentative of the real atmosphere, the analytic solutions which are readily obtained display, to a remarkable extent, the qualitative features of more realistic, less soluble models. If the potential vorticity is non-zero but uniform, the Boussinesq approximation enables us to again produce an analytic solution. Solutions for specific temperature distributions and the formation of realistic surface fronts in these solutions have been described in some detail in Hoskins (1971) (later referred to as H). We also give the methods of solution when non-Boussinesq effects, smooth changes in potential vorticity, and crude models of latent heat and surface friction are included in the problem.

The application of the deformation model to the formation of upper tropospheric fronts and their associated jet streams is discussed. The troposphere-stratosphere system is modelled by two perfect fluids of different potential vorticities, with the internal boundary (tropopause) sloping such that there is zero temperature gradient along the upper boundary. Again, the solutions have been given in H.

The second situation was first described by R. T. Williams. In 1967, he published a numerical study of the finite-amplitude development of a baroclinic wave independent of the meridional direction. Williams integrated the Boussinesq equations and found that the ageostrophic motions distorted the finite-amplitude wave. A phenomenon similar to an atmospheric surface cold front formed. The frontogenesis was initiated by the shear in the meridional velocity of the developing wave acting on the temperature distribution in that direction, i.e., by the horizontal shear effect.

This model is studied theoretically (Section 5b). We show, making only the assumption of geostrophic balance in the zonal direction, that the full nonlinear problem may be solved analytically. The solution agrees well with the numerical one and, in particular, exhibits frontogenesis at the surface.

Thus, two fundamental mechanisms are shown to trigger frontogenesis. In each case the quasi-geostrophic equations describe an intensification of the temperature contrasts and an increase in relative vorticity until the scaling assumptions underlying these equations are breaking down. In both models of surface fronts, when the relative vorticity is no longer small compared with the Coriolis parameter, the ageostrophic circulation becomes important, producing the tilt of the front and upgliding motion up this slope. The vertical deformation field soon dominates and produces at a rigid boundary a tendency to form discontinuities in a finite time. In Section 6 this collapse process is studied in detail. In the final stages, potential temperature and long-front velocity are constant on the same plane surfaces of constant slope. These material surfaces move together at a constant speed determined by the motion away from the collapse region and discontinuities must form at the boundary in a finite time. In the upper tropospheric front, the tropopause acts like a flexible boundary but, unlike the surface front, discontinuities do not appear.

However, actual discontinuities are not formed in the atmosphere. The above models eventually break down, but this does not occur first in the assumption of geostrophic cross-front balance. The Richardson numbers in the frontal region decrease as the intensity of the front increases until they become so small that overturning and consequent mixing must occur. By this time, large relative vorticities and strong fronts may be formed.

The most elegant and, in the authors' view, most revealing approach to the problems discussed is the Lagrangian one given in the main body of the paper. However, the reader with limited time may find it easier to read the approach given in the Appendix. There, the Eulerian equations of motion for a general model are studied. If this is done, the "Lagrangian" Sections 3b, 3d and 5b may be largely ignored.

2. Equations, coordinates and vorticity results

a. The equations of motion with a new vertical coordinate

We introduce a Cartesian coordinate system fixed in the surface of the earth and use the primitive equations for an inviscid, adiabatic, perfect gas with ratio of specific heats γ and pressure p, density ρ and potential temperature θ; values having zero subscripts are typical of conditions at the earth's surface, introduced for dimensional convenience. We make the traditional quasi-static approximation (Eliassen and Kleinschmidt, 1957, p. 20) of ignoring the vertical acceleration and the horizontal component of the earth's rotation. Thus, we assume hydrostatic balance in the vertical. As vertical coordinate we use a certain function of pressure rather than p itself, i.e.,

$$z=\left[1-\left(\frac{p}{p_0}\right)^{(\gamma-1)/\gamma}\right]\frac{\gamma}{\gamma-1}H_s, \tag{2.1}$$

where the scale height $H_s=p_0/(\rho_0 g)$. It should be noted that increments in "pseudo height" z are connected to increments in physical height h by

$$\theta dz=\theta_0 dh. \tag{2.2}$$

Defining

$$z_a=\frac{\gamma}{\gamma-1}H_s\approx 28\text{ km}, \tag{2.3}$$

we have that the pseudo height z is bounded above by $z=z_a$. For an adiabatic atmosphere $(\theta=\theta_0)$, $z=h$ exactly. For a real atmosphere, θ normally increases upward and the physical height exceeds z. The relations for the ICAO standard atmosphere and for adiabatic and isothermal atmospheres are shown in Fig. 3 (reproduced from H). A sounding will almost always produce a curve between the adiabatic and isothermal curves shown. Thus, to a good first approximation, z can be considered as physical height over the troposphere. Since the slopes of surfaces of constant pressure are $O(10^{-4})$, they are horizontal to a good approximation. The words "horizontal" and "height" will often be used to refer to

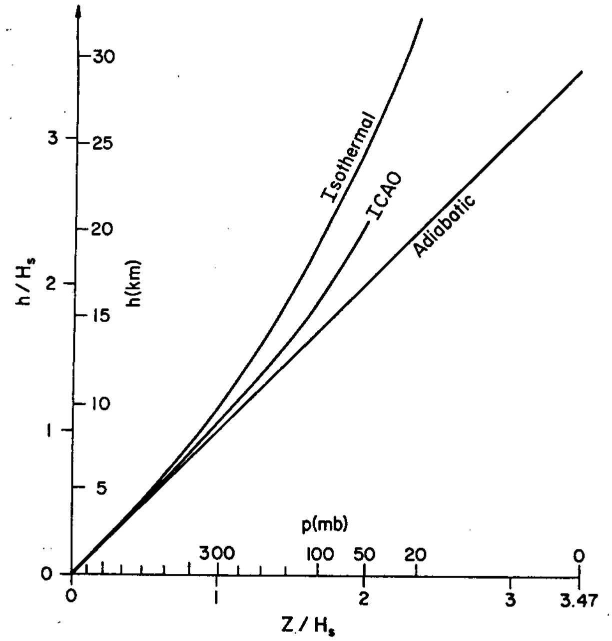

FIG. 3. The relation between physical height (h) and z for the ICAO standard atmosphere and for isothermal and adiabatic atmospheres. Pressure is also marked on the z axis (every 100 mb below 300 mb and every 50 mb between 300 and 100 mb).

surfaces z=constant, and to the coordinate z, respectively. Though not exact, the terminology is suggestive and useful.

We also introduce a pseudo density

$$r(z)=\rho_0(p/p_0)^{1/\gamma}=\rho_0(1-z/z_a)^{1/\gamma-1}, \tag{2.4}$$

which is a known function of z or pressure only. In an adiabatic atmosphere, r would be the true density. Hydrostatic balance requires that

$$rdz=-dp/g=\rho dh. \tag{2.5}$$

The equations of motion are

$$D\mathbf{u}/Dt+f\mathbf{k}\times\mathbf{u}+\nabla_h\phi=0, \tag{2.6}$$

$$\nabla\cdot(r\mathbf{v})=0, \tag{2.7}$$

$$D\theta/Dt=0, \tag{2.8}$$

$$\partial\phi/\partial z=(g/\theta_0)\theta, \tag{2.9}$$

where:

$w=Dz/Dt=-(Dp/Dt)/[gr(z)]$

$\mathbf{k}$=unit vertical vector

$\mathbf{u}=(u,v,0)$

$\mathbf{v}=(u,v,w)=\mathbf{u}+w\mathbf{k}$

$\nabla_h=(\partial/\partial x,\partial/\partial y,0)$

$\nabla=(\partial/\partial x,\partial/\partial y,\partial/\partial z)=\nabla_h+\mathbf{k}\dfrac{\partial}{\partial z}$

ϕ=geopotential$=gh$

f=Coriolis parameter, here taken as constant.

Note that, with this vertical coordinate, the hydrostatic relation (2.9) assumes a simple and convenient form. However, the known function $r(z)$ appears both in the definition of the vertical velocity w and in the equation for conservation of mass (2.7). This particular form of the equations has apparently not been previously used systematically in analytical studies, but has certain advantages.

Eq. (2.7) may be rewritten as

$$\nabla\cdot\mathbf{v}=w/[\gamma H_s(1-z/z_a)]. \tag{2.10}$$

Clearly, if $1-z/z_a$ is not small (certainly true below 100 mb), and if the height scale for w is much smaller than the scale height, then the right-hand side of (2.10) may be neglected and the Boussinesq equations are obtained. Although we shall make it from time to time, this approximation is not vital for our analysis as will be shown later by some examples.

From the definitions of z and w in terms of pressure, it is clear that the upper boundary condition is

$$w=0 \text{ at } z=z_a.$$

At the surface of a smooth earth we should have $D\phi/Dt=0$. But surface pressure varies only within about $\pm5\%$. Also, if U is a speed characteristic of meso- and large-scale atmospheric systems, we have $U\ll$speed of sound. Then, to a reasonable approximation, as is often done in the p system of coordinates, the bottom condition may be written as

$$w=0 \quad\text{at}\quad z=0.$$

More recent studies have shown that the error introduced here is negligible.

b. Cross-front geostrophic balance

It has been found observationally that in large-scale atmospheric flow there is always an approximate balance between the pressure and Coriolis forces. In phenomena such as jets and fronts, the length scale in one horizontal direction (cross-front) is much smaller than that in the other (long-front), and the horizontal velocity vector has only a small component in the cross-front direction. It is found that there is approximate geostrophic balance in the cross-front direction. This fact was used by Sawyer (1956) and Eliassen (1959, 1962) in their theoretical studies of atmospheric frontogenesis. In this numerical work showing the production of a front, Williams (1967) found that cross-front geostrophic balance was well satisfied. It should be remarked that geostrophic balance in the long-front direction of a well-developed jet or front is not a good approximation.

We now present a non-dimensionalization of our equations which shows the consistency of considering a straight front with geostrophic balance across it. Consider a frontal situation in which there are gradients

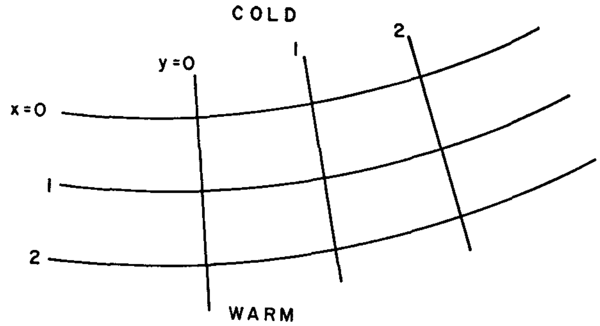

FIG. 4. The horizontal coordinate axes.

of physical quantities in the cross-front direction much larger than those in the long-front direction. Choose x coordinate lines in the long-front direction, with x increasing toward warmer air, and y coordinate lines everywhere in the horizontal direction of maximum temperature gradient such that (x,y,z) is a set of right-handed, orthogonal, curvilinear coordinates (Fig. 4). Since our coordinates are not rectangular Cartesian, extra terms, $-v^2/R$, uv/R, occur in the x and y accelerations respectively, where R is the local radius of curvature of the front.

We non-dimensionalize using

$$\left.\begin{array}{l} x=l\tilde{x},\quad y=L\tilde{y},\quad z=h\tilde{z},\quad t=T\tilde{t},\quad u=U\tilde{u} \\ v=V\tilde{v},\quad w=W\tilde{w},\quad \theta=\theta_0+\Theta\tilde{\theta},\quad \phi=gz+\Phi\tilde{\phi} \end{array}\right\}. \quad (2.11)$$

The equations of motion (2.6)–(2.9) may then be written:

$$\alpha\beta^2\tilde{D}\tilde{u}-\tilde{v}+\left(\frac{\Phi}{l}\frac{1}{fV}\right)\frac{\partial\tilde{\phi}}{\partial\tilde{x}}-\alpha\frac{l}{R}\tilde{v}^2=0, \quad (2.12)$$

$$\tilde{D}\tilde{v}+\frac{1}{\alpha}\tilde{u}+\frac{1}{\alpha}\left(\frac{\Phi}{l}\frac{1}{fV}\right)\left(\frac{l}{U}\frac{V}{L}\right)\frac{\partial\tilde{\phi}}{\partial\tilde{y}}+\frac{l}{R}\tilde{u}\tilde{v}=0, \quad (2.13)$$

$$\frac{\partial\tilde{u}}{\partial\tilde{x}}+\left(\frac{l}{U}\frac{V}{L}\right)\frac{\partial\tilde{v}}{\partial\tilde{y}}+\left(\frac{l}{U}\frac{W}{h}\right)\frac{1}{r}\frac{\partial}{\partial\tilde{z}}(r\tilde{w})-\frac{l}{R}\tilde{u}=0, \quad (2.14)$$

$$\tilde{D}\tilde{\theta}=0, \quad (2.15)$$

$$\frac{\Phi}{h}\frac{\partial\tilde{\phi}}{\partial\tilde{z}}=\frac{g\Theta}{\theta_0}\tilde{\theta}, \quad (2.16)$$

where

$$\tilde{D}=\frac{l}{U}\left(\frac{1}{T}\frac{\partial}{\partial\tilde{t}}+\frac{U}{l}\tilde{u}\frac{\partial}{\partial\tilde{x}}+\frac{V}{L}\tilde{v}\frac{\partial}{\partial\tilde{y}}+\frac{W}{h}\tilde{w}\frac{\partial}{\partial\tilde{z}}\right),$$

$\alpha=V/fl$ is a dimensionless measure of wind shear across the front, and $\beta=U/V$ a characteristic tangent of the angle between the horizontal velocity vector and the y axis. In a frontal zone we expect

$$1/T\approx U/l\approx W/h\gtrsim V/L, \quad \alpha=O(1),$$

but $l/L\leqslant\beta\ll 1$. If $R\gg\alpha l$, curvature terms may be neglected. The smallness of β suggests that the acceleration term in (2.12) may be neglected and the equation may be approximated by a statement of geostrophic balance. Then Eqs. (2.12) and (2.16) give $fV\approx\Phi/l\approx gh\Theta/(l\theta_0)$. In Eqs. (2.13) and (2.14) only the curvature terms may be neglected. We then obtain the equations for a straight front with the approximation of geostrophic balance across the front. The consistency of this balance in any model may be checked by comparing the neglected cross-front acceleration with the cross-front pressure gradient. If the front becomes extremely sharp and α becomes large enough that $\alpha\beta^2$ is no longer negligible, we must expect that the approximation will break down. As we move away from the frontal zone to where $y=O(L)$, U/V may not be small, but geostrophic balance still holds because $V/fL\ll 1$.

For reference, we give the approximated equations in dimensional form as used hereafter:

$$Dv/Dt+fu+\partial\phi/\partial y=0, \quad (2.17)$$

$$\nabla\cdot(r\mathbf{v})=0, \quad (2.18)$$

$$D\theta/Dt=0, \quad (2.19)$$

where

$$\theta(g/\theta_0)=\partial\phi/\partial z, \quad (2.20)$$

$$fv=\partial\phi/\partial x. \quad (2.21)$$

$$D/Dt=\partial/\partial t+\mathbf{v}\cdot\nabla. \quad (2.22)$$

c. Circulation and potential vorticity assuming cross-front geostrophic balance

Consider a material circuit A and define its circulation to be

$$C(t)=\oint_A v\,dy. \quad (2.23)$$

From the equations of motion

$$\frac{d}{dt}(C+fS)=\frac{g}{\theta_0}\oint_A \theta\,dz, \quad (2.24)$$

where $S(t)$ is the area of the projection of the circuit into a horizontal surface. This is the form taken by Kelvin's circulation theorem, known in meteorological literature as V. Bjerknes' first circulation theorem (Eliassen and Kleinschmidt, p. 14). For a material circuit on a "horizontal" (constant pressure) boundary or in a surface of constant potential temperature, the right-hand side is zero and the "absolute circulation" is conserved. In our frame moving with the earth, this is interpreted that change in circulation can be caused only by horizontal shrinkage or expansion of the circuit. The production of absolute circulation is positive if the temperature distribution is such that cyclonic flow around the circuit would result in warm air rising and cold air sinking. Although (2.24) is formally equivalent to the full Kelvin's circulation theorem, inspection of (2.23) shows that under the cross-front balance approximation, changes in $\oint_A(udx)$ are neglected compared with those in $\oint_A(vdy)$.

It is readily shown from (2.17)–(2.22)) that Ertel's potential vorticity under the balance assumption is

$$q=[-(\partial v/\partial z)\partial\theta/\partial x+(f+\partial v/\partial x)\partial\theta/\partial z]/r, \quad (2.25)$$

and is conserved following fluid particles, i.e.,

$$Dq/Dt=0. \quad (2.26)$$

From (2.25) is it seen that changes in $\partial u/\partial y$ and $(\partial u/\partial z)\partial\theta/\partial y$ are neglected compared with changes in $\partial v/\partial x$ and $(\partial v/\partial z)\partial\theta/\partial x$, respectively. Unlike the quasi-geostrophic form of potential vorticity, q involves horizontal temperature gradients and components of vorticity. The importance of including these terms was stressed by Reed and Sanders (1953) in their demonstration of how potential vorticity may be used as a tracer in upper tropospheric fronts.

There is a deduction concerning frontogenesis which can be made directly from the potential vorticity equation. Substituting for v and θ, from (2.20) and (2.21), in (2.25), we have

$$(f^2+\partial^2\phi/\partial x^2)\partial^2\phi/\partial z^2-(\partial^2\phi/\partial x\partial z)^2=(fg/\theta_0)rq, \quad (2.27)$$

where q is conserved following fluid particles and is normally positive everywhere. Thus, we can consider (2.27) as an equation for ϕ with rq some unknown but positive function of position. It is an elliptic equation of the Monge-Ampère type. A theorem of Heinz (1961) says that provided $\partial\phi/\partial x$ and $\partial\phi/\partial z$ remain bounded everywhere and rq has continuous spatial derivatives up to the second order, then singularities in the second derivatives of ϕ are possible only on boundaries. This tells us that provided v and θ remain bounded, discontinuities in v or θ can occur only on a boundary or at a discontinuity in potential vorticity or its first or second derivatives. This important result is in agreement with the observation that really strong fronts occur only near the earth's surface or near the tropopause separating stratospheric and tropospheric air which have very different potential vorticities. It proved helpful in formulating the models described later.

We define the component of absolute vorticity normal to a pressure surface, hereafter loosely called the vertical component of absolute vorticity, as

$$\zeta=f+\partial v/\partial x, \quad (2.28)$$

and the Richardson number

$$\mathrm{Ri}=(g/\theta)(\partial\theta/\partial h)/(\partial v/\partial h)^2$$
$$=(g/\theta_0)(\partial\theta/\partial z)/(\partial v/\partial z)^2. \quad (2.29)$$

Then (2.25) may be rewritten as

$$\zeta/f=1/\mathrm{Ri}-rq/(f\partial\theta/\partial z). \quad (2.30)$$

When a strong front is formed, q, r and f retain their original magnitudes but $\partial\theta/\partial z$ becomes large. Then

$$\mathrm{Ri}\approx f/\zeta. \quad (2.31)$$

Thus, in strong fronts the Richardson numbers will be small and there will be a tendency for small-scale instability and clear air turbulence to set in.

3. Horizontal deformation and the formation of surface fronts

a. The basic model

A simple deformation field independent of height may be written as

$$u=-\alpha x, \quad v=\alpha y, \quad (3.1)$$

where α is possibly a function of time and $\alpha/f\ll 1$, $d\alpha/dt\leqslant O(\alpha^2)$. We consider the action of this velocity field on a potential temperature distribution initially independent y and so widespread in the x direction that the thermal wind is negligible. We expect that this potential temperature distribution will remain independent of y but will be concentrated in the x direction.

We seek a solution

$$\left.\begin{aligned} u&=-\alpha x+u'(x,z,t)\\ v&=\alpha y+v'(x,z,t)\\ w&=w(x,z,t)\\ \phi&=f\alpha xy-(\alpha^2+d\alpha/dt)y^2/2+\phi'(x,z,t)\\ \theta&=\theta(x,z,t)\end{aligned}\right\} \quad (3.2)$$

where u', v', w and horizontal gradients in θ are negligible everywhere initially and for all time at infinity. The additional y-dependent term in ϕ is necessary to ensure the consistency of the y dependence of the model.

Since we anticipate that we shall form "fronts" oriented in the y direction, we use the equations of motion with the assumption of geostrophic balance in the x direction [Eqs. (2.17)–(2.22)]. By inserting (3.2) into these equations it may be verified that the y-dependent terms cancel and we have a consistent problem involving only two space dimensions. From this point on we shall often refer to "motion in the x, z plane." Since the y dependence is so trivial, this is a convenient way to refer to the motion of the point of intersection of a material line in the y direction with a plane y=constant. We shall also refer to lines on which some quantity is constant. Strictly speaking, these are the intersections of surfaces on which this quantity is constant and the plane y=constant.

Our interest is in the region near the origin in x and there the approximation of geostrophic balance in the x direction is a good one. However, at extremely large x, the x acceleration implied by the basic deformation field is not strictly negligible. If this is accounted for (see Appendix), the equations with x geostrophic balance are obtained except that ϕ is now the geopotential plus $(\alpha^2-d\alpha/dt)x^2/2$. This is a trivial correction term and does not influence the circulation and potential vorticity results of Section 2c.

b. Lagrangian study

We start by identifying three quantities which are constant or vary in a known manner following "material particles" as they move in the x, z plane. These characterize the essential dynamics of the system in simple terms. We will later introduce a transformation of coordinates which exploits these quantities and is the mathematical innovation which allows significant progress toward analytic solution of what is otherwise a hopelessly complex, nonlinear problem.

Clearly, one quantity which is conserved as a "material particle" moves in the x, z plane is the potential temperature θ.

Another which varies in a known manner is

$$M = v' + fx.$$

To see this we apply Kelvin's circulation theorem (2.24) to the circuit $A_1B_1B_2A_2$ (Fig. 5), where A_1B_1, A_2B_2 are lines of fluid particles parallel to the y axis and of equal length L. Since u and v are independent of y, and $\partial u/\partial y$ is independent of position, these lines remain parallel to the y axis, but each is extended

$$\frac{dL}{dt} = \alpha L. \tag{3.3}$$

This may be integrated to give

$$L = L_0 e^{\beta(t)}, \tag{3.4}$$

where

$$\beta = \int_0^t \alpha(t')dt'.$$

The curves A_1A_2, B_1B_2 are parallel to each other, and θ and the tangential velocity have the same value at corresponding points on each. Thus, they make no contribution to the net circulation or to the generation term $\oint \theta dz$. Then Kelvin's circulation theorem gives

$$\frac{D}{Dt}\{v_2'L + \tfrac{1}{2}\alpha L^2 - (v_1'L + \tfrac{1}{2}\alpha L^2) + fL(x_2 - x_1)\} = 0,$$

i.e.,

$$\frac{D}{Dt}\{M_1 L\} = \frac{D}{Dt}\{M_2 L\}. \tag{3.5}$$

But as $x \to \infty$, $v' \to 0$, so there

$$\frac{D(Me^{\beta})}{Dt} = f\frac{Dx}{Dt} + \alpha M = -\alpha fx + \alpha M = 0.$$

Choosing A_2B_2 sufficiently distant for this to hold, we deduce that

$$\frac{DM}{Dt} + \alpha M = 0, \tag{3.6}$$

$$M = M_0 e^{-\beta}, \tag{3.7}$$

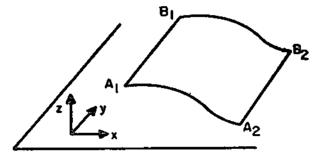

FIG. 5. A circuit for Kelvin's circulation theorem.

following *any* fluid particle. These relations may also be readily deduced directly from the equations of motion. However, this approach via Kelvin's circulation theorem shows the dynamical significance of the quantity.

Consideration of a circuit like $A_1B_1B_2A_2$ shows that $M_1 = M_2$ is the condition that the circulation round the circuit vanishes. Thus, the absolute vorticity vector lies in the surfaces M = constant. Furthermore,

$$\partial M/\partial x = f + \partial v/\partial x = \zeta,$$
$$\partial M/\partial z = \partial v/\partial z,$$

where $\partial v/\partial z$ is the component of vorticity in a surface of constant pressure, perpendicular to the y axis, multiplied by a known function of pressure. Thus, M is a "streamfunction" for the absolute vorticity in the x, z plane. An alternative interpretation was provided by Eliassen (1962) who suggested that M be called the absolute momentum of a particle.

It is also useful to introduce the quantity X such that

$$M = fX. \tag{3.8}$$

Thus,

$$X = x + v'/f.$$

Since we have $X = x$ in the initial state, (3.6) and (3.7) imply that

$$DX/Dt = -\alpha X, \quad X = X_0 e^{-\beta}.$$

Thus, if a particle moved with the geostrophic deformation velocity, its x coordinate would be X, and so we call X the geostrophic coordinate. However, particles do not move with the deformation velocity. Since M is a streamfunction of the absolute vorticity, geostrophic coordinate lines must crowd together in regions of large vorticity.

We have two quantities M and θ whose variation following a fluid particle is known for all time and between them we have the thermal wind relation (assumption of geostrophic balance in the x direction)

$$f\partial M/\partial z = (g/\theta_0)\partial\theta/\partial x.$$

To specify the motion completely, we need one further Lagrangian property. This must be provided by conservation of mass. Using our vertical coordinate, the mass of a "volume" of fluid dV is equal to $r(z)dV$. The simple y dependence implies that mass conservation may be stated as rdV = constant following a fluid volume in the x, z plane. Consider the volume between two neighboring θ surfaces $\theta - \Delta\theta/2$, $\theta + \Delta\theta/2$, two neighboring M surfaces $M - \Delta M/2$, $M + \Delta M/2$ which in the basic state were $M_0-\Delta M_0/2$, $M_0+\Delta M_0/2$ (where $\Delta M_0=\Delta M e^{\beta}$), and of length $L=L_0 e^{\beta}$ in the y direction. This volume is

$$dV=L\Delta M\Delta\theta\left[\frac{\partial(M,\theta)}{\partial(x,z)}\right]^{-1}=L_0\Delta M_0\Delta\theta\left[\frac{\partial(M,\theta)}{\partial(x,z)}\right]^{-1}$$

$$=\text{constant}\times\left[\frac{\partial(M,\theta)}{\partial(x,z)}\right]^{-1};$$

thus, mass conservation implies

$$\frac{1}{r}\frac{\partial(M,\theta)}{\partial(x,z)}=q \tag{3.9}$$

is constant following a fluid particle in the x, z plane. In fact, substituting for M in (3.9), it is seen that q is precisely Ertel's potential vorticity under the geostrophic balance assumption [Eq. (2.25)]. This is consistent as the only ingredient in the conservation of potential vorticity which is not contained in the circulation theorem, and conservation of potential temperature is mass conservation.

Thus, using D to denote the derivative moving with a particle in the x, z plane, the equations are

$$\left.\begin{array}{l} DM=-\alpha M\\ D\theta=0\\ Dq=0\end{array}\right\}, \tag{3.10}$$

where

$$rq=\partial(M,\theta)/\partial(x,z),\quad f\partial M/\partial z=(g/\theta_0)\partial\theta/\partial x.$$

A somewhat different constraint follows from these relations together with the upper and lower boundary conditions. A surface of material particles is marked by a constant value of $Xe^{-\beta}$, where $X=M/f$ is the geostrophic coordinate introduced above. The mass contained between two such surfaces and the rigid boundaries $z=0$, H must be constant. Remembering the uniform extension parallel to Oy, we have

$$e^{\beta}\int_0^H r(z)[x(X_1,z,t)-x(X_2,z,t)]dz =F(X_1e^{-\beta})-F(X_2e^{-\beta}), \tag{3.11}$$

where $F(X)$ is a function which depends only on the initial conditions. We will consider only situations in which the initial temperature contrasts are so spread out that $\partial v'/\partial z$ is negligibly small and

$$X\sim x \quad \text{at} \quad t=0.$$

Furthermore, we suppose that this remains true as $x\rightarrow\infty$ for all subsequent time. In this case

$$F(X)=X\int_0^H r(z)dz,$$

and (3.11) becomes

$$\int_0^H r(z)v'(X,z,t)dz=0, \tag{3.12}$$

where the integration is in a surface of constant X. This condition and the thermal wind equation enable us to infer the complete long-front velocity field $v'(x,z,t)$ from a knowledge only of horizontal temperature gradients $(\partial\theta/\partial x)(x,z,t)$.

c. The model with zero potential vorticity

We now consider the special case in which everywhere M and θ surfaces coincide, i.e., the potential vorticity is identically zero. This does not imply that any motion must be irrotational, but it does imply that the circulation in surfaces of constant θ is zero for all time. The reasons for introducing this model are that it can be solved very easily and that the method of solution suggests how to attack the general problem. The solution simply shows many of the characteristics which are exhibited by solutions of the general problem. The model has some importance in its own right since one of the features of well-developed fronts and their associated cloud systems is that the wet bulb potential temperature is approximately constant up the frontal slope. As the absolute vorticity vector is usually oriented approximately along the frontal slope, the effective potential vorticity based on the wet bulb potential temperature is approximately zero. Since the idea of this subsection is to produce simple results, we shall make the Boussinesq approximation by ignoring dr/dz in the mass conservation equation, and shall consider a fluid between boundaries at $z=0$ and $z=H$.

Suppose that initially $\theta=\theta_i(x)$ where $d\theta/dx$ is so small that $\partial v'/\partial z$ is negligible and $X=x$. Since θ is conserved and $X=X_0e^{-\beta}$ following a fluid particle (where X_0 = initial x position),

$$\theta(x,z,t)=\theta_i[X(x,z,t)e^{\beta(t)}]=\Theta(X,t), \tag{3.16}$$

say, a known function of both X and time. Then,

$$q=\frac{\partial(X,\theta)}{\partial(x,z)}=0$$

is satisfied identically, with X and θ both being constant on lines with slope

$$\frac{\partial X}{\partial x}\bigg/\frac{\partial X}{\partial z}=\frac{\partial X}{\partial x}\bigg/\left(\frac{g}{f^2\theta_0}\frac{\partial\theta}{\partial x}\right)=\frac{f^2\theta_0}{g}\bigg/\frac{\partial\Theta}{\partial X}. \tag{3.17}$$

Thus, at any time t, the lines on which θ and X are constant are straight and of known slope.

To study the effects of mass conservation which under the Boussinesq approximation is volume conservation, we refer to Fig. 6 where CD is at large

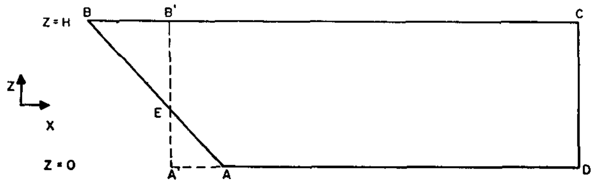

FIG. 6. Mass conservation in the zero potential vorticity model.

enough x such that it is moving with the deformation velocity, AB is a line on which θ and X are constant, and A'B' is where this line would have been if all points on it had moved with the deformation velocity. According to Eq. (3.12), we must have

$$\text{area ABCD} = \text{area A'B'CD}.$$

Therefore, the point E must be at $z=H/2$ and so the mid-point of each line on which X and θ are constant is at the position it would have reached if the whole line had moved with the horizontal deformation velocity, i.e., it has x coordinate X. From (3.17), therefore, a general point on the line has known x coordinate

$$x=X-(g/f^2\theta_0)z'\partial\Theta/\partial X, \qquad (3.18)$$

where $z'=z-H/2$. On this line, we know θ and

$$v'=f(X-x)=(g/f\theta_0)z'\partial\Theta/\partial X. \qquad (3.19)$$

Therefore, at any time t we know v' and θ as a function of position. The amount of frontogenesis as determined by gradients in v' and θ is easily calculated; thus, for example, the vertical component of absolute vorticity is

$$\zeta=f\partial X/\partial x=f[1-(g/f^2\theta_0)z'(\partial^2\Theta/\partial X^2)]^{-1}. \qquad (3.20)$$

The determination of the velocities in the x, z plane which must perform the development described by (3.16) and (3.18) is not essential to the problem. However, using

$$u=\frac{Dx}{Dt}=-\alpha X-(g/f^2\theta_0)(\alpha z'+w)\partial\Theta/\partial X, \qquad (3.21)$$

the continuity equation may be integrated up lines $X=$constant to give

$$w=-\left(\frac{\alpha g}{f^2\theta_0}\frac{\partial^2\Theta}{\partial X^2}\right)\frac{H^2/4-z'^2}{1-(g/f^2\theta_0)z'(\partial^2\Theta/\partial X^2)}. \qquad (3.22)$$

Thus the "vertical circulation" (u,w) is known as a function of position.

We note some general properties of the problem and its solution.

1) Time has become a parameter; it is not necessary to find the solution for $t<T$ in order to determine that at T, but only to specify the total geostrophic deformation $e^{\beta(T)}$ that has occurred.

2) It is useful to use X and z as independent variables. The nonlinearity of the problem reduces to the simple graphical exercise of finding $\theta(x,z)$ given $\theta(X)$ and $x(X,z)$.

3) The frontogenesis problem of determining v' and θ at time t has separated from the problem of finding u and w.

4) Provided the rate of deformation α remains finite, infinite vorticity and associated discontinuities in velocity and temperature occur in a *finite* time, since in (3.20) $\partial^2\Theta/\partial X^2 \propto e^{2\beta(t)}$. It can be seen that this "collapse" occurs first on the boundaries. The singularity occurs not in the problem as viewed using X, z, but in the transformation $x(X,z)$.

5) Below $z=H/2$, the largest vertical vorticity at any time is on the line on which $\partial^2\Theta/\partial X^2$ is a minimum, which was the line on which, initially, $\partial^2\theta_i/\partial x^2$ was a minimum.

6) There is upward motion or downward motion according as $\partial^2\Theta/\partial X^2$ is negative or positive.

7) In a region of initially uniform temperature gradient, there is no vertical motion, no vertical vorticity generation and hence no real frontogenesis.

8) From 5), 6) and 7), we may deduce that, in this model, frontogensis will tend to occur on the lower boundary toward the warm side of a temperature contrast.

9) At a boundary, (3.21) may be rewritten as

$$u=-\alpha x-(2\alpha/f)v',$$

which on differentiation becomes

$$\partial u/\partial x=-\alpha-(2\alpha/f)\partial v'/\partial x. \qquad (3.23)$$

The first term on the right-hand side is the basic horizontal deformation, while the second is the vertical deformation associated with the induced ageostrophic circulation. For vertical vorticities large compared with f, the latter dominates.

10) Consistency of the balance approximation demands that

$$|(\partial/\partial z)(Du/Dt)|\ll|f\partial v'/\partial z|,$$

which may be shown to imply that

$$\zeta/f\ll(2\alpha/f)^{-2}.$$

Typically, since $\alpha/f\approx10^{-1}$, we must have $\zeta_{\max}\ll25f$. This restriction is so weak that the model could thus consistently predict frontal vorticities as large as are ever observed.

11) Setting $q=0$ in (2.30), we find $\mathrm{Ri}f/\zeta$. Thus, as the vertical vorticity increases, the Richardson number decreases until instability (e.g. Kelvin-Helmholtz) sets in and neglected mixing effects must be important. We may expect this to happen before $\mathrm{Ri}=0.1$, i.e., $\zeta_{\max}=10f$. Hence, this provides the real restriction on the model, not the balance approximation. Comment

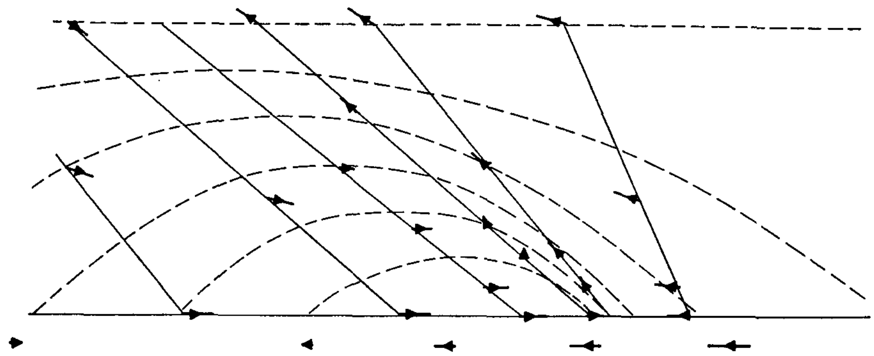

FIG. 7. Deformation model with zero potential vorticity (lower half domain). Continuous and broken lines are isolines of potential temperature and long-front velocity, respectively. Arrowed lines are the velocity vectors drawn on the same scale as the basic deformation velocity shown beneath the lower surface.

4) should be amended to state that there is a tendency to form discontinuities in a finite time.

To show the realistic appearance of the solutions of this simple model, we exhibit in Fig. 7 a solution corresponding to an inverse tangent form for the initial potential temperature distribution. The total geostrophic deformation is such that $\lambda_{\max}=5f$.

d. Non-zero potential vorticity

As suggested by the previous section, we now consider the general problem using as independent variables X and Z, where X is the geostrophic coordinate $(=x+v'/f)$ and $Z=z$. The latter notation is used so as to simplify the transformation of coordinates. Equivalent independent variables have previously been used by Eliassen (1962) to simplify his equation for vertical circulation in frontal zones. Formally, we have

$$\partial/\partial x=(\partial X/\partial x)\partial/\partial X, \tag{3.24}$$

$$\partial/\partial z=(\partial X/\partial z)\partial/\partial X+\partial/\partial Z. \tag{3.25}$$

Now,

$$\partial X/\partial x=1+(1/f)\partial v'/\partial x=\zeta/f,$$

and (3.24) thus gives

$$\partial v'/\partial x=(\zeta/f)\partial v'/\partial X.$$

Adding f to both sides and rearranging, we find

$$\zeta/f=[1-(1/f)\partial v'/\partial X]^{-1}. \tag{3.26}$$

Since $\partial X/\partial z=(1/f)\partial v'/\partial z$, (3.25) gives

$$\partial v'/\partial z=(\zeta/f)\partial v'/\partial Z.$$

But

$$\partial\theta/\partial x=(\zeta/f)\partial\theta/\partial X,$$

and so the thermal wind equation becomes

$$f\partial v'/\partial Z=(g/\theta_0)\partial\theta/\partial X. \tag{3.27}$$

Thus, the simplicity of this basic thermal wind relationship is preserved. An alternative statement of this fact is as follows: There exists a function Φ such that

$$fv'=\partial\Phi/\partial X,\quad (g/\theta_0)\theta=\partial\Phi/\partial Z, \tag{3.28}$$

precisely analogous to the geopotential in physical space. It is easily seen that

$$\Phi=\phi'+v'^2/2. \tag{3.29}$$

The Jacobian of the transformation is ζ/f and so it is mathematically valid as long as the vertical component of absolute vorticity is positive and finite.

From (3.14),

$$rq=(\zeta/f)[\partial(M,\theta)/\partial(X,Z)].$$

But $M=fX$. Therefore

$$rq=\zeta\partial\theta/\partial Z. \tag{3.30}$$

Consider a cylinder in the direction of the absolute vorticity vector and bounded by θ and $\theta+\Delta\theta$. Neglecting non-Boussinesq effects, from (3.30), conservation of potential vorticity says that the horizontal absolute circulation about this cylinder is proportional to the vertical height of the cylinder. Using (3.26), (3.30) may be written as

$$rq=f(\partial\theta/\partial Z)[1-(1/f)\partial v'/\partial X]^{-1}. \tag{3.31}$$

In the initial state, if we denote a particle's position by (x_0,z_0), then, since v' is negligible, we have

$$r(z_0)q=f\partial\theta/\partial z_0. \tag{3.32}$$

But since z_0 is not physical height, we may define a pseudo Brunt-Väisälä frequency

$$N^2=(g/f\theta_0)r(z_0)q=(g/\theta_0)\partial\theta/\partial z_0.$$

If at $z_0=0$ the potential temperature is $\theta_1(x_0)$, then, integrating (3.32), we have

$$\theta(x_0,z_0)=\theta_1(x_0)+\frac{1}{f}\int_0^{z_0} r(z_0')q(x_0,z_0')dz_0'. \tag{3.33}$$

We may thus consider q, N^2 and z_0 as functions of x_0 and θ provided q is non-zero everywhere. As a material particle moves, $X = x_0 e^{-\beta(t)}$ and θ is conserved. Since q is also conserved, at any subsequent time q, N^2 and z_0 may be considered as known functions of X and θ. Also, the potential temperature at any horizontal boundary is a known function of X only.

Thus, using (3.28) we may rewrite (3.31):

$$\frac{1}{f^2}\frac{\partial^2\Phi}{\partial X^2}+\frac{f\theta_0}{g}\frac{1}{r(Z)q(X,\partial\Phi/\partial Z)}\frac{\partial^2\Phi}{\partial Z^2}=1. \quad (3.34)$$

The boundary conditions are:

$$\partial\Phi/\partial X \to 0 \quad \text{as} \quad X\to\pm\infty, \quad (3.35)$$

$$\partial\Phi/\partial Z = (g/\theta_0)\theta_1(X) \quad \text{on} \quad Z=0, \quad (3.36)$$

and, assuming $\partial\theta/\partial z_0$ is everywhere finite in the initial state,

$$\partial\Phi/\partial Z = (g/\theta_0)\theta_2(X) \quad \text{on} \quad Z=z_a. \quad (3.37)$$

From (3.33), we must have

$$\theta_2(X)=\theta_1(X)+\frac{1}{f}\int_0^{z_a} r(z_0)q(x_0,z_0)dz_0. \quad (3.38)$$

This problem may be conveniently restated in terms of the potential temperature θ by taking the Z derivative of (3.34):

$$\frac{1}{f^2}\frac{\partial^2\theta}{\partial X^2}+\frac{\partial}{\partial Z}\left[\frac{f\theta_0}{g}\frac{1}{r(Z)q(X,\theta)}\frac{\partial\theta}{\partial Z}\right]=0, \quad (3.39)$$

with

$$\partial\theta/\partial X\to 0 \quad \text{as} \quad X\to\pm\infty, \quad (3.40)$$

$$\theta=\theta_1(X) \quad \text{on} \quad Z=0, \quad (3.41)$$

$$\theta=\theta_2(X) \quad \text{on} \quad Z=z_a. \quad (3.42)$$

Introducing N^2 and $\mu(X,Z,\theta)=r(z_0)/r(Z)$, (3.39) has the alternative form

$$\frac{\partial^2\theta}{\partial X^2}+\frac{\partial}{\partial Z}\left[\mu(X,Z,\theta)\frac{f^2}{N^2(X,\theta)}\frac{\partial\theta}{\partial Z}\right]=0. \quad (3.43)$$

Given the solution to the problem for θ, v' may be determined by integration along geostrophic coordinate lines (X=constant) of the thermal wind relation (3.27), using (3.12) to determine the constant of integration. The position of each fluid particle is then

$$(x,z)=[X-f^{-1}v'(X,Z),Z]. \quad (3.44)$$

The deformation problem has thus been reduced to a simple form in which time occurs only indirectly. It determines the total geostrophic deformation $e^{\beta(t)}$ which provides the scale of the functions q, θ_1 and θ_2. The only non-linearities are the dependence of q on θ in (3.39), and the transformation back to physical space which is, however, easily performed graphically. The time-dependent problem for v' and θ, as it is formulated above, has completely separated from that for the velocity in the x, z plane. One method for looking at motions in this plane is to solve the problem at two times and relate the positions of a fluid particle in the two solutions. Alternatively, we may return to the equations of motion and obtain an equation for the pseudo streamfunction ψ of the flow in the x, z plane (such that $ru'=\partial\psi/\partial z$, $rw=-\partial\psi/\partial x$) as was done by Sawyer (1956) and Eliassen (1962) in terms of the instantaneous distributions of v' and θ. In the Appendix, the equations for a model which includes the deformation model are transformed using the geostrophic coordinate. The equations obtained above and the equation for the x, z pseudo streamfunction are found. This latter equation is [from Eqs. (A25) and (A34)]

$$\frac{\partial}{\partial X}\left(\frac{q}{f}\frac{\partial\psi}{\partial X}\right)+\frac{\partial}{\partial Z}\left(\frac{f^2\theta_0}{g}\frac{1}{r}\frac{\partial\psi}{\partial Z}\right)=-2\alpha\frac{\partial\theta}{\partial X}. \quad (3.45)$$

As stated in the Appendix, integration over a surface S bounded by a closed streamline shows that round this streamline the circulation is counterclockwise, viewed from the negative y axis, when $\alpha\int_s(\partial\theta/\partial X)dS$ is positive. In a deformation model ($\alpha>0$), we thus expect a tendency for a thermodynamically direct circulation, with warm air rising and cold air subsiding.

In X, Z space, ζ/f increases to ∞ and the associated approach to discontinuities in velocity and temperature corresponds merely to $\partial\theta/\partial Z$ decreasing to 0. Also, since fX is a streamfunction of the absolute vorticity, X coordinate lines will be crowded together in a region of high vorticity, i.e., X is a boundary-layer type coordinate for fronts. Therefore, accurate solutions exhibiting frontogenesis should be obtainable, however strong the front.

e. *Uniform potential vorticity model*

The simplest model is $N^2(X,\theta)=\text{constant}=N_0^2$, say. This implies that in the initial state, θ is a linear function of z. From (2.2), this corresponds to $\theta\propto(\text{physical height})^{\frac{1}{2}}$. In this section we shall make the Boussinesq-type approximation

$$\mu(X,Z,\theta)=r(z_0)/r(Z)\equiv 1. \quad (3.46)$$

If we had used the Boussinesq equations from the beginning, we would have derived (3.43) with condition (3.46). The approximation should be valid provided particles do not move a vertical distance comparable to H_s. Since we have a problem in which there are no discontinuities in q or any of its derivatives, we can expect to form strong fronts only at the lower and upper boundaries. We are interested only in front formation at the lower boundary as any similar phenomenon at the upper boundary is a product of the unrealistic condition that $\partial\theta/\partial z_0$=constant up to the top, and is not physically interesting. Because of our interest only in the development near the surface, we impose a "rigid" lid at $z=H$ below that otherwise implied at $z=z_a$. The approximations made in this model will all be reconsidered in later sections.

The equation for θ may be stated as

$$\frac{\partial^2\theta}{\partial X^2}+\frac{f^2}{N_0^2}\frac{\partial^2\theta}{\partial Z^2}=0. \quad (3.47)$$

It is convenient to nondimensionalize using the height H and the pseudo Brunt-Väisälä frequency M_0. Denoting dimensionless quantities by tildes, we set

$$X=(N_0H/f)\tilde{X},\quad Z=H\tilde{Z},\quad \theta=(\theta_0/g)N_0^2H\tilde{\theta},\quad v'=N_0H\tilde{v}.$$

The equation and the boundary conditions (3.40)–(3.42), with the condition (3.38) that the system developed from an initial state of zero v', may be conveniently restated as

$$\partial^2\tilde{\theta}/\partial\tilde{X}^2+\partial^2\tilde{\theta}/\partial\tilde{Z}^2=0, \quad (3.48)$$

$$\left.\begin{array}{c}\tilde{\theta}(\tilde{X},1)=1+\tilde{\vartheta}(\tilde{X}/\tilde{L})\\ \tilde{\theta}(\tilde{X},0)=\tilde{\vartheta}(\tilde{X}/\tilde{L})\\ \tilde{\theta}\rightarrow\tilde{Z}+\tilde{\vartheta}(\pm\infty)\quad\text{as}\quad\tilde{X}\rightarrow\pm\infty\end{array}\right\}. \quad (3.49)$$

The time-dependence occurs only in determining the length scale L of the basic horizontal temperature distribution.

We now set

$$\tilde{\theta}=\tilde{Z}+\tilde{\vartheta}(\tilde{X}/\tilde{L})+\theta^*. \quad (3.50)$$

A general temperature distribution $\tilde{\vartheta}(x)$ is the sum of an even function of x and an odd function of x, say $\tilde{\vartheta}_1(x)$ and $\tilde{\vartheta}_2(x)$, respectively. To find θ_1^*, the even part of θ^* forced by $\tilde{\vartheta}_1$, we introduce the Fourier sine transform of the odd function $\partial\tilde{\vartheta}_1/\partial x$:

$$F_1(k)=\left(\frac{2}{\pi}\right)^{\frac{1}{2}}\int_0^\infty \tilde{\vartheta}_1'(x)\sin kx\,dx,$$

and use the Fourier cosine transformation of θ_1^*. Similarly, to determine θ_2^*, the odd part of θ^* forced by $\tilde{\vartheta}_2$, we denote the Fourier cosine transform of $\partial\tilde{\vartheta}_2/\partial x$ by $F_2(k)$ and use the sine transform of θ_2^*. Combining the solutions we find that

$$\tilde{\theta}(\tilde{X},\tilde{Z},\tilde{L})=\tilde{Z}+\tilde{\vartheta}_1(\tilde{X}/\tilde{L})+\tilde{\vartheta}/\tilde{L})+\left(\frac{2}{\pi}\right)^{\frac{1}{2}}\int_0^\infty\left[1-\frac{\cosh k(\tilde{Z}-\frac{1}{2})}{\cosh k/2}\right]\times\frac{F_1(k\tilde{L})\cos k\tilde{X}-F_2(k\tilde{L})\sin k\tilde{X}}{k}dk. \quad (3.51)$$

Using the thermal wind relation and the potential vorticity equation (3.31), it is easily seen that

$$\tilde{v}'=\left(\frac{2}{\pi}\right)^{\frac{1}{2}}\int_0^\infty\frac{\sinh k(\tilde{Z}-\frac{1}{2})}{\cosh k/2}\times\frac{F_1(k\tilde{L})\sin k\tilde{X}+F_2(k\tilde{L})\cos k\tilde{X}}{k}dk. \quad (3.52)$$

Since the dimensionless coordinate $\tilde{x}$ is simply $\tilde{X}-\tilde{v}'$, the frontogenetic problem for this model has been solved.

Under the Boussinesq approximation, $\psi^*=\psi/r$ is the proper streamfunction for the x, z motion, and its equation when non-dimensionalized by $\psi^*=(\alpha NH^2/f)\tilde{\psi}$ is

$$\partial^2\tilde{\psi}/\partial\tilde{X}^2+\partial^2\tilde{\psi}/\partial\tilde{Z}^2=-2\partial\tilde{\theta}+/\partial\tilde{X}\ \text{with}\ \tilde{\psi}=0\ \text{on}\ \tilde{Z}=0,1. \quad (3.53)$$

The solutions corresponding to the odd and even forcing may easily be found by using transforms as above. The result is

$$\tilde{\psi}=-\left(\frac{2}{\pi}\right)^{\frac{1}{2}}\times\int_0^\infty\frac{(\tilde{Z}-\frac{1}{2})\sinh k(\tilde{Z}-\frac{1}{2})-\frac{1}{2}\tanh k/2\cosh k(\tilde{Z}-\frac{1}{2})}{k\cosh k/2}\times[F_1(k\tilde{L})\sin k\tilde{X}+F_2(k\tilde{L})\cos k\tilde{X}]dk. \quad (3.54)$$

The solutions for particular initial potential temperature distributions and geostrophic deformations may be obtained by numerical quadrature. We evaluate the two integrals for $\partial\tilde{\theta}/\partial\tilde{X}$ and $\partial\tilde{\theta}/\partial\tilde{Z}$ for a 31×17 grid, $0\leqslant\tilde{X}\leqslant 5.4L$, $0\leqslant\tilde{Z}\leqslant\frac{1}{2}$, using a 96 point Gaussian method routine, truncating the integrals at $k=48$. The derivative quantities ζ/f, $\partial\tilde{\theta}/\partial\tilde{x}$, $\partial\tilde{\theta}/\partial\tilde{z}$, Ri$[=(\partial\tilde{\theta}/\partial\tilde{z})\times(\partial\tilde{\theta}/\partial\tilde{x})^{-2}]$ may then be evaluated directly. We know $\tilde{\theta}$ on $\tilde{Z}=0$ and clearly from (3.52) $\tilde{v}'=0$ on $\tilde{Z}=\frac{1}{2}$. Then $\tilde{\theta}$ and $\tilde{v}'$ are determined in $0\leqslant\tilde{Z}\leqslant\frac{1}{2}$ by numerical integration of $\partial\tilde{\theta}/\partial\tilde{Z}$ and $\partial\tilde{v}'/\partial\tilde{Z}=\partial\tilde{\theta}/\partial\tilde{X}$ using the trapezium rule. Since $\partial\tilde{\theta}/\partial\tilde{Z}$, $\partial\tilde{\theta}/\partial\tilde{X}$, $\tilde{\theta}$ and $\tilde{v}'$ all have obvious symmetry properties about $\tilde{X}=0$ and $\tilde{Z}=\frac{1}{2}$, we obtain the solution for a region $-4.5L\leqslant\tilde{X}\leqslant 4.5L$ of the fluid $(0\leqslant\tilde{Z}\leqslant 1)$.

Finally, we obtain $\tilde{x}=\tilde{X}-\tilde{v}'$ for each grid point. The transformation to physical space may be done graphically by drawing the lines $\tilde{X}$=constant in physical space, and drawing contours of quantities noting that their values are known at the intersection of these geostrophic coordinate grid lines with the grid lines $\tilde{Z}=\tilde{z}$=constant. The drawing of contours in frontal areas with their large gradients is simplified as the $\tilde{X}$ grid lines are close together in these regions of large vorticity.

Solutions for particular odd and even temperature distributions have been given in *H*. There the formation of sloping frontal regions with maximum gradients in velocity and temperature at the surface is described in detail. For these surface fronts, and quite generally we expect, as L decreases $\partial\tilde{\theta}/\partial\tilde{Z}$ tends to zero somewhere. This implies that ζ/f increases to ∞ there. Hence, given any two-dimensional initial temperature distribution acted on by a large-scale horizontal deformation field, we expect that there will be a tendency to form frontal discontinuities in a finite time.

f. Comparison with quasi-geostrophic theory

If we had used quasi-geostrophic theory to attack this problem (e.g., Williams and Plotkin, 1968) the mathematical problem could have been stated as

$$\left.\begin{array}{l} \partial^2\phi'/\partial x^2+(f^2/N_0^2)\partial^2\phi'/\partial z^2=f^2 \\ \partial\phi'/\partial x\rightarrow 0 \quad \text{as} \quad x\rightarrow\pm\infty \\ \partial\phi'/\partial z=(g/\theta_0)\theta_1(x/L) \quad \text{on} \quad z=0 \\ \partial\phi'/\partial z=(g/\theta_0)\theta_2(x/L) \quad \text{on} \quad z=H \end{array}\right\}. \tag{3.55}$$

We recall that the geostrophic relations are

$$(g/\theta_0)\theta=\partial\phi'/\partial z, \quad fv'=\partial\phi'/\partial x.$$

Without making the restrictive assumptions of quasi-geostrophic theory, we have obtained equations which are identical to these with ϕ', x, z replaced by Φ, X, Z. Thus, our balanced model must give the same values of v' and θ as quasi-geostrophic theory, but these values are predicted at $(X-v'/f, z)$ rather than at (X,z). Thus, our theory only predicts a distortion of the quasi-geostrophic solution, but this distortion is vital in the description of frontogenesis. In particular, the vertical component of absolute vorticity is

$$\left.\begin{array}{l} \zeta=f[1-f^{-1}\partial v'/\partial X]^{-1} \text{ in the balanced model} \\ \zeta=f[1+f^{-1}\partial v'/\partial x] \text{ in quasi-geostrophic theory} \end{array}\right\}.$$

Therefore, where quasi-geostrophic theory predicts $\zeta=2f$, the balance theory predicts that the vorticity has become infinite. Also, if quasi-geostrophic theory gives $\zeta=0$, the balance theory gives $\zeta=f/2$.

This overestimate of the development of negative relative vorticity and underestimate of that of positive relative vorticity by quasi-geostrophic theory may be understood by referring to the vertical vorticity equation at the ground. For simplicity, we make the "Boussinesq" and x geostrophic balance approximations. The vorticity equation is

$$(D/Dt)\partial v/\partial x=(f+\partial v/\partial x)\partial w/\partial z.$$

In the quasi-geostrophic approximation, $\partial v/\partial x$ is ignored compared with f on the right-hand side. Clearly this is not valid in a model of frontogenesis, and also its effect must be as described above.

g. Refinements of the model

1) NON-BOUSSINESQ

If we do not make the Boussinesq-type approximation (3.46), the nondimensional N^2=constant problem for $\tilde{\theta}$ becomes

$$\partial^2\tilde{\theta}/\partial\tilde{x}^2+(\partial/\partial\tilde{z})(\mu\partial\tilde{\theta}/\partial\tilde{z})=0, \tag{3.56}$$

with boundary conditions (3.49). Since the original height of a fluid particle is $z_0=H[\tilde{\theta}(\tilde{X},\tilde{Z})-\tilde{\theta}(\tilde{X},0)]$, $\mu=r(z_0)/r(H\tilde{Z})$ is a function of $\tilde{\theta}$, and this problem is nonlinear. However, it is clearly solvable numerically by relaxation. We replace the boundary condition at infinity by one at $\tilde{X}=\pm 1.5$ to obtain

$$\tilde{\theta}(\pm 1.5\tilde{Z},)=\tilde{Z}+\tilde{\theta}(\pm 1.5/\tilde{L}). \tag{3.57}$$

As a control experiment we use this numerical method to solve the Boussinesq problem with $\tilde{\theta}(\tilde{X}/\tilde{L})=\pi^{-1}\tan^{-1}\tilde{x}/0.185$. The solution is almost identical to that analytic one exhibited in H. Numerical solution of the non-Boussinesq problem shows little difference: μ varies from 1.12 on the warm side to 0.90 on the cold side; the patterns of $\tilde{v}'$ and $\tilde{\theta}$ are very similar but frontogenesis proceeds rather slower at the ground and more quickly at the lid; and the maximum vertical component of absolute vorticity averaged over the lowest level is $2.8f$ and over the highest level $3.8f$ as compared with $3.2f$ in the control. [This is consistent with the vorticity equation derived from (2.6)–(2.9).] It may be easily seen that the non-Boussinesq term causes a decrease in vorticity in rising air and an increase in descending air. Thus, near a lower boundary where vorticity is decreased by descending air and increased by ascending air, we expect that the vorticity is more uniform than predicted by Boussinesq theory. The reverse is true at the lid.

2) NON-UNIFORM POTENTIAL VORTICITY.

The Boussinesq equation for a general smooth distribution of potential vorticity, when nondimensionalized as above, is

$$\partial^2\tilde{\theta}/\partial\tilde{X}^2+(\partial/\partial\tilde{Z})(\nu^2\partial\tilde{\theta}/\partial\tilde{Z})=0, \tag{3.58}$$

where $\nu^2=N^2/N_0^2$ is a known function of $\tilde{X}$, $\tilde{\theta}$. As above, this may be solved by relaxation. An integration with ν^2 varying from 1 at the surface to 6 at the lid shows, as expected, frontogenesis at the surface slightly decreased and that at the lid greatly decreased.

3) LATENT HEAT.

In this work we consider that latent heat release is not crucial in frontogenesis. However, it is clear that it must have an important modifying effect. Numerical models with a general circulation model by Manabe *et al.* (1970) have clearly indicated that, in a moist model, there are stronger upward motions and increased gradients at fronts.

To crudely model latent heat release, following Eliassen (1959), we consider it as a heat source in an otherwise dry adiabatic atmosphere, i.e.,

$$D\theta/Dt=E. \tag{3.59}$$

In the Appendix it is shown that the geostrophic coordinate may be introduced and the previous equations obtained except that now

$$Dq/Dt=\zeta\partial E/\partial Z. \tag{3.60}$$

If we assume that the solution is little altered by the inclusion of this heating, we may estimate the increase in q, postulate a new distribution of potential vorticity, and resolve the problem. Use of this method confirms that latent heat release produces larger upward motions and increased frontogenesis.

Approaching the problem rather differently, one of the observed effects of the cloud and rain associated with fronts is that there is little stability for motion along vortex lines. The potential vorticity based on the wet bulb potential temperature is approximately zero. Hence, the zero potential vorticity model described earlier has some relevance in this case. The solution exhibited (Fig. 7) was very similar to those of the constant N^2 model (see H), but the total deformation required to achieve a given maximum vorticity is less. Thus, again, the enhancing effect on frontogenesis is demonstrated.

4) SURFACE FRICTION.

We again consider this as a perturbation on our previous control model. We model the effect of a surface boundary layer by imposing at $z=0$ the Ekman layer suction

$$w=(\delta/2)(\zeta-f). \tag{3.61}$$

The height risen between $\tilde{L}=0.25$ and $\tilde{L}=0.185$ by a fluid particle at the lower boundary may then be estimated from the solutions at these times. Rather than solve with $\tilde{\theta}$ known on this boundary, it is more convenient to interpolate to $\tilde{Z}=0$ using the values of $\partial\tilde{\theta}/\partial\tilde{Z}$ in the lowest grid of the control experiment.

Taking $\alpha=2.10^{-5}S^{-1}$, $\delta=150$ m, the numerical solution of the problem produces a similar distribution of $\tilde{v}$, $\tilde{\theta}$, but the frontogenesis is reduced. The maximum value of y is reduced from $3.2f$ to $2.4f$. In the surface boundary layer at a front there is increased convergence but above there is a compensating divergence whose effect is frontolytic.

4. A discontinuous potential vorticity model and upper tropospheric fronts

In 1955, Reed published his observational study of a remarkable upper tropospheric front. Before this there had been classical studies of the polar jet front by Bjerknes and Palmèn (1937) and Bergeron (1937). The latter, noting the subsidence at the front, introduced the terminology "katafront." The first theory of the jet stream formation was that of Rossby [University of Chicago (1947)] who evoked large-scale mixing. The confluence theory of jet stream intensification was proposed by Namias and Clapp (1949). Many investigators commented on the vertical motion in the vicinity of a jet stream. However, Reed's use of potential vorticity as a tracer enabled him to produce, for the first time, a very complete picture of frontogenesis in the upper troposphere. He showed that the tropopause, with stratospheric air of large potential vorticity on one side and tropospheric air on the other, folded back on itself. A thin layer of stratospheric air penetrated deep down into the troposphere taking on the form of a frontal region. During this process, the jet stream intensified somewhat. Although this was a remarkable case, it has since become clear that most of the phenomena Reed observed are characteristic of upper tropospheric fronts. A detailed study of five similar cases has been made by Reed and Danielsen (1959), and Danielsen (1968) has produced more evidence of the folding of the tropopause. In the 1960's there has been some interest in the vertical motion near jet streams as this plays an important part in tropospheric-stratospheric exchange (e.g., Newell, 1963).

The general deformation model, which we reduced to a simple form in Section 3, was used there only in a uniform potential vorticity model. The solutions exhibited phenomena similar to surface fronts. The similar "frontal" formation at the lid was found not to affect the dynamics near the surface. However, in this section we are interested in modeling the formation of fronts away from the surface. Because of the large static stability of the stratospheric air above, the tropopause often acts almost as a rigid lid for tropospheric motions. Clearly, this cannot be considered an explanation of upper tropospheric frontogenesis, but it encourages us to extend our model. We shall consider a large-scale deformation field acting on a system composed of fluid of one potential vorticity (the troposphere) under fluid of a larger potential vorticity (the stratosphere). We recall from Section 2c that at a discontinuity in potential vorticity we expect the possibility of forming large gradients.

To keep the model simple, we shall make the Boussinesq approximation. By doing this we shall tend to overestimate vorticity formed by upward motion and underestimate that formed by downward motion. Thus, if we succeed in producing any phenomena similar to the upper tropospheric fronts observed, we shall have underestimated the amount of frontogenesis there.

a. The equations

We denote the upper and lower regions by the subscripts 2 and 1, respectively. Using the geostrophic coordinate X, the equations are

$$\left.\begin{aligned}\partial^2\theta_2/\partial X^2+(f^2/N_2^2)\partial^2\theta_2/\partial Z^2=0\\ \partial^2\theta_1/\partial X^2+(f^2/N_1^2)\partial^2\theta_1/\partial Z^2=0\end{aligned}\right\}. \qquad (4.1)$$

We demand that $\partial\theta_2/\partial X$ and $\partial\theta_1/\partial X\rightarrow 0$ as $|X|\rightarrow\infty$. We take the lowest boundary as $Z=0$, the highest boundary $Z=H$, and the internal boundary (tropopause) as $Z=h(X)$. Since the X coordinate of fluid particles changes with the geostrophic deformation rate, if the tropopause is initially a single-valued function of X, it remains so. We note that this does not imply that it must remain a single-valued function of x. We may write the potential temperatures on $Z=0$, h, H as $\vartheta_1(X/L)$, $\vartheta_t(X/L)$, $\vartheta_2(X/L)$. As before, time only appears indirectly. It determines the total geostrophic deformation and hence the length L. This problem is shown in Fig. 8a. Let $h_0(X/L)$ be the initial height of the tropopause, now with geostrophic coordinate X. Since we consider the initial state to be one of negligible v', we must have

$$\left.\begin{aligned}\vartheta_t=\vartheta_1+N_1^2(\theta_0/g)h_0\\ \vartheta_2=\vartheta_t+N_2^2(\theta_0/g)(H-h_0)\end{aligned}\right\}. \qquad (4.2)$$

Thus, only two of the functions h_0, ϑ_1, ϑ_2, ϑ_t may be specified arbitrarily.

To specify the problem uniquely we require a matching condition across the tropopause. Integration of Eqs. (4.1) over the area bounded by the circuit ABCD in Fig. 8a gives

$$0=[\partial\theta/\partial X]_1^2dZ+[(f^2/N^2)\partial\theta/\partial Z]_1^2dX. \qquad (4.3)$$

Here $[F]_1^2\equiv F_2-F_1$. But the continuity of θ implied by $\theta_1=\vartheta_t(X/L)=\theta_2$ at the tropopause gives

$$0=[\partial\theta/\partial X]_1^2dX+[\partial\theta/\partial Z]_1^2dZ. \qquad (4.4)$$

Combining (4.3) and (4.4), we have

$$\frac{\partial\theta_2/\partial Z}{\partial\theta_1/\partial Z}=\frac{N_2^2[1+(N_1^2/f^2)(dh/dX)^2]}{N_1^2[1+(N_2^2/f^2)(dh/dX)^2]}, \qquad (4.5)$$

where dh/dX is the slope of the tropopause in the X, Z plane.

From the work in Section 3 we have

$$N^2=[g/(f\theta_0)]\zeta\partial\theta/\partial Z, \qquad (4.6)$$

and thus

$$\partial v'/\partial X=f-(gf/\theta_0)N^{-2}\partial\theta/\partial Z. \qquad (4.7)$$

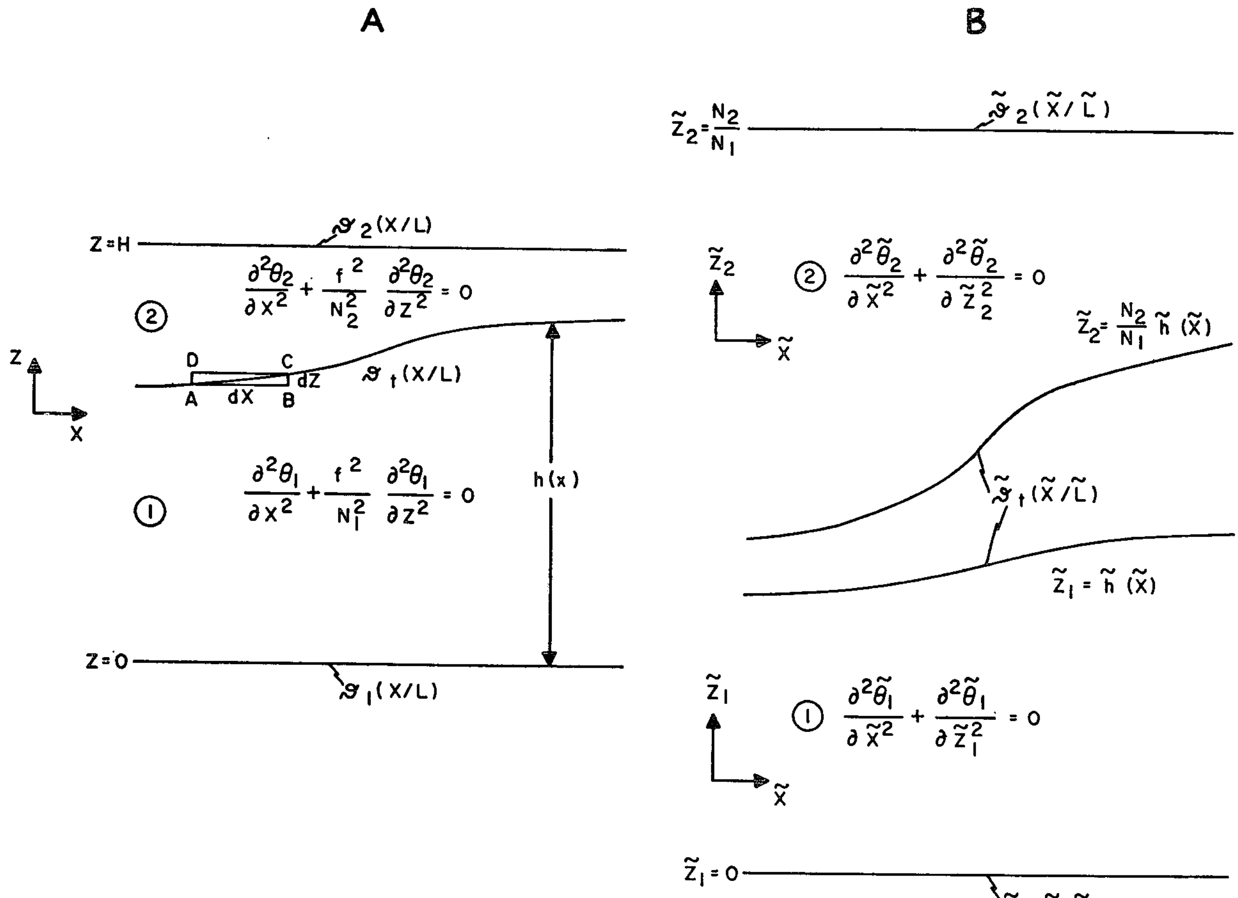

FIG. 8. Discontinuous potential vorticity deformation model: The problem. A, dimensional; B, nondimensional.

Also

$$\partial v'/\partial Z=[g/(f\theta_0)]\partial\theta/\partial X. \tag{4.8}$$

We see that (4.3), and hence (4.5), are merely conditions for continuity in v' across the tropopause. From (4.6), (4.5) may be written as

$$\frac{\zeta_1}{\zeta_2}=\frac{1+(N_1^2/f^2)(dh/dX)^2}{1+(N_2^2/f^2)(dh/dX^2)}. \tag{4.9}$$

When the tropopause has zero slope, $(\partial\theta_2/\partial Z)(\partial\theta_1/\partial Z)^{-1}=N_2^2N_1^{-2}$ and $\zeta_1=\zeta_2$. However, since $N_2>N_1$, when the slope is non-zero, $(\partial\theta_2/\partial Z)(\partial\theta_1/\partial Z)^{-1}<N_2^2N_1^{-2}$, and $\zeta_2>\zeta_1$. The vertical component of absolute vorticity is larger on the stratospheric side of the tropopause than on the tropospheric side. This effect should be important when $dh/dX\approx f/N_2$.

The mathematical problem posed has certain unusual features. We have essentially Laplace's equation for θ in the two regions, with θ known around the boundaries of both regions. However, the position of the common boundary is unknown. The matching condition (4.5) across this boundary is a function of its slope. For convenience, we now nondimensionalize the equations in such a manner that the governing equations in both regions is Laplace's equation. We set

$$\left.\begin{aligned}\theta=(\theta_0/g)N_1^2H\tilde{\theta},\quad v'=N_1H\tilde{v},\quad X=(N_1H/f)\tilde{X}\\ \tilde{Z}=H\tilde{Z}_1\text{ in (1)},\quad\text{and}\quad Z=(H/\nu)\tilde{Z}_2\text{ in (2)}\end{aligned}\right\}, \tag{4.10}$$

where $\nu=N_2/N_1$. The nondimensional model is shown in Fig. 8b.

To keep our model simple we require that there should be no potential temperature gradient on the lid. In nondimensional terms this implies

$$d\tilde{\vartheta}_1/\partial\tilde{X}=(\nu^2-1)d\tilde{h}o/\partial\tilde{h}\tilde{X}.$$

b. *The method of solution*

Since the mathematical problem is not a standard one, various techniques for numerical solution were tried. The one described here was successful in giving solutions to the particular problems displayed in H and to others.

As was done in the numerical work described in the previous section, we replace the boundary condition at infinity by one at $\tilde{X}=\pm1.5$:

$$\left.\begin{aligned}\tilde{\theta}_1(\pm1.5,\tilde{Z})&=\tilde{\vartheta}_1(\pm1.5/\tilde{L})+\tilde{Z}_1\\ \tilde{\theta}_2(\pm1.5,\tilde{Z})&=\tilde{\vartheta}_2(\pm1.5/\tilde{L})-\nu(\nu-\tilde{Z}_2)\end{aligned}\right\}. \tag{4.11}$$

We also impose that the values of $\tilde{h}$ at $\tilde{X}=\pm1.5$ are fixed at the initial values relevant to those fluid lines:

$$\tilde{h}(\pm1.5)=\tilde{h}_0(\pm1.5/\tilde{L}). \tag{4.12}$$

Solutions obtained using this boundary condition will tend to have less tropopause movement than those using the exact condition.

The method of attack is to fix the tropopause and relax toward the solutions of Laplace's equation in both fluids with the correct boundary conditions except at the tropopause. There we impose (4.5) but we demand only that $\tilde{\theta}_1=\tilde{\theta}_2$. We do not specify $\tilde{\theta}_1=\tilde{\vartheta}_t=\tilde{\theta}_2$. After a certain number of steps we move the tropopause to a new position such that the values of the potential temperature on the tropopause are likely to be nearer the correct ones. We then repeat the process. If this double relaxation procedure converges, then it converges to the solution of the problem, subject to round-off error.

The details of the numerical scheme are given in Hoskins (1970).

c. *Some solutions*

The solutions of Experiments 1, 2 and 3, as described in H, all exhibit upper air fronts, jet streams, and the various stages in the formation of a tongue of stratospheric air descending into the troposphere. However, the ageostrophic convergence at the upper air front does not suggest a tendency to form infinite vorticity as exists at surface fronts. We now consider under what conditions such a tendency may exist. Since the vorticity is always larger on the stratospheric side of the tropopause, we need only consider the stratosphere. Suppose that we know the tropopause height in the $\tilde{X}$, $\tilde{Z}_2$ plane. If there is a tongue of stratospheric air, the position must be much as in the schematic diagram of Fig. 9a. The governing equation is Laplace's equation and we may assume that $\tilde{\theta}_2$ is known on the boundaries. Experiments 1, 2 and 3 all have potential temperature increasing monotonically along the tropo-

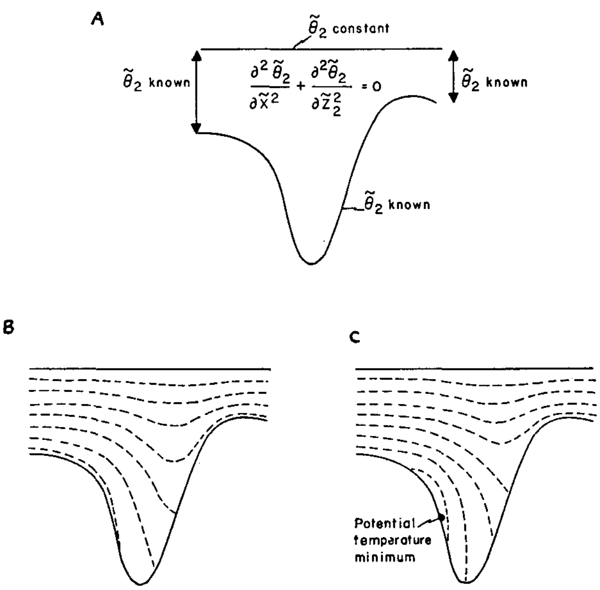

FIG. 9. Stratospheric descent: A, the mathematical problem; B, tropopause potential temperature monotonically increasing; C, potential temperature minimum on the tropopause.

pause. For any such problem, the potential temperature distribution must be similar to that in Fig. 9b. Since $f^{-1}\zeta=\nu(\partial\tilde{\theta}_2/\partial\tilde{Z}_2)^{-1}$, the vorticity is clearly large in the tongue and hence when transformed into physical space it must be narrow. We should expect that the vorticity is approximately proportional to ν and to the depth of the tongue. However, since the tropopause must always have finite slope, in the $\tilde{X}$, $\tilde{Z}_2$ plane we can never obtain $\partial\tilde{\theta}_2/\partial\tilde{Z}_2\rightarrow 0$, i.e., $\zeta/f\rightarrow\infty$.

Now suppose that the potential temperature has a minimum on the tropopause on the "cold" side of the tongue. The potential temperature distribution in the $\tilde{X}$, $\tilde{Z}_2$ plane is shown schematically in Fig. 9c. It is seen that $\partial\tilde{\theta}_2/\partial\tilde{Z}_2\rightarrow 0$ is then possible. In fact, a minimum or maximum anywhere on the tongue, apart from a minimum at the base of the tongue, introduces the possibility of a tendency to infinite vorticity.

Reed (1955) noted a mass of extremely cold air on the cold side of the temperature transition in the upper troposphere and his diagrams show a potential temperature minimum on the tropopause toward the cold side of the tongue. If the air on the cold side of the tongue is to have very small baroclinicity, there must be such a minimum on the cold side of the tongue. Therefore, this is the physically interesting case. However, experiments in which the tropopause potential temperature has this minimum indicate that a minimum in tropopause height tends to occur there. Thus, we have found no tendency to form infinite vorticity at upper air fronts.

5. A horizontal shear model

In this section we describe an analytic study of a model which was investigated numerically by Williams (1967). He considered a Boussinesq fluid with uniform static stability, bounded by two rigid horizontal planes. The fluid had a uniform temperature gradient in the unbounded y direction and a corresponding geostrophic x wind linearly increasing with height. This is the basic state for the simplest example of the classical phenomenon of baroclinic instability. According to quasi-geostrophic theory, a perturbation in the form of an infinitesimal Eady wave should grow indefinitely, preserving its shape, and drawing on the infinite source of available potential energy associated with the infinite temperature contrast in the y direction. Williams posed, as initial conditions for his model, the basic state perturbed by the most unstable Eady wave. His integrations showed that horizontal shears develop much as quasi-geostrophic theory suggests. The warm southerly winds and cold northerly winds form temperature gradients in the x direction (east). However, when the perturbation has grown to finite amplitude, ageostrophic motions cause a distortion of the dynamical picture in which a realistic surface front is formed. The basic y-temperature gradient is much smaller than those produced in the x direction. He found that there is a tendency to produce frontal discontinuities in a finite time.

In Sections 5a, b we attack a more general problem and then restrict ourselves to Williams's problem. The solution of this model shows that the formation of a realistic surface front may be initiated by the horizontal shear mechanism though rather extreme velocities seem to be required.

a. The basic model

We shall study a model in which

$$\left.\begin{aligned}\theta&=-\theta_0 g^{-1}s^2 y+\theta'(x,z,t)\\ \phi&=-s^2 y(z-h)+\phi'(x,z,t)\end{aligned}\right\}, \tag{5.1}$$

and all other dependent variables are independent of y. Here $s=(-g\theta_0^{-1}\partial\theta/\partial y)^{\frac{1}{2}}$ has the dimensions of a frequency and is a constant along with h. Then

$$u_g=s^2 f^{-1}(z-h).$$

The zonal (x direction) geostrophic wind increases linearly with height.

We make the approximation of geostrophic balance in the x direction. Insertion of (5.1) into Eqs. (2.17)–(2.22) shows that the y dependence posed is consistent. As in the deformation model, we may refer to motion in the x, z plane and lines in this plane.

b. Lagrangian study and the transformation

The potential temperature is conserved following a fluid particle. We also apply Kelvin's circulation theorem (2.24) as before (Fig. 5).

This time there is no extension in the long-front direction, i.e.,

$$\frac{DL}{Dt}=0. \tag{5.2}$$

The theorem gives

$$\left\{\frac{D}{Dt}M-s^2 z\right\}\bigg|_1=\left\{\frac{D}{Dt}M-s^2 z\right\}\bigg|_2. \tag{5.3}$$

The generation term $s^2 z$ arises because the values of $g\theta/\theta_0$ at corresponding point on A_1A_2, B_1B_2 differ by $s^2 L$. At large distances we have the boundary condition

$$u\rightarrow\frac{s^2}{t}(z-h),\quad v\rightarrow 0\quad \text{as } x\rightarrow\infty. \tag{5.4}$$

Changing the value of the constant h in this expression would merely involve adding a uniform geostrophic velocity to our solution. From (5.3), (5.4) we have, for *all* particles,

$$\frac{D}{Dt}M=s^2(z-h). \tag{5.5}$$

Thus, the change in M following a fluid particle is determined purely by the height of the particle. As in the deformation model, this equation could have been derived directly from the equations of motion. Again, M is a streamfunction for the absolute vorticity in the x, z plane.

The direct application of mass conservation to this problem is not trivial, and so we prefer to use the conservation of potential vorticity [(2.25), (2.26)], which may be written as

$$\frac{Dq}{Dt}=0, \quad \text{where} \quad rq=\frac{\partial(M,\theta')}{\partial(x,z)}. \tag{5.6}$$

For comparison with (3.15) for the deformation model, we restate our equations using D to denote the derivative moving with a particle in the x, z plane; thus, we have

$$\left.\begin{aligned} DM&=s^2(z-h)\\ D\theta'&=(\theta_0/g)s^2v\\ Dq&=0\end{aligned}\right\}, \tag{5.7}$$

where $rq=\partial(M,\theta')/\partial(x,z)$, $f\partial M/\partial z=(g/\theta_0)\partial\theta'/\partial x$.

As before, we introduce X such that $M=fX$. Then

$$X=x+v/f. \tag{5.8}$$

In an initial state with negligible v, we have $X=x$. Changes in X are given by

$$DX/Dt=s^2f^{-1}(z-h). \tag{5.9}$$

Since this is the geostrophic x velocity, if a particle moved from the initial state with only the geostrophic velocity, its x coordinate would be X. We again call X the geostrophic coordinate.

We now transform our independent variables to X and $Z(=z)$. The process is entirely analogous to the transformation for the deformation model. We have

$$\partial/\partial x=(\zeta/f)\partial/\partial X, \tag{5.10}$$

$$\partial/\partial z=(g/f\theta_0)(\zeta/f)(\partial\theta'/\partial X)\partial/\partial X+\partial/\partial Z, \tag{5.11}$$

where

$$\zeta=f+\partial v/\partial x=f[1-(1/f)\partial v/\partial X]^{-1}. \tag{5.12}$$

Also, if

$$\Phi'=\phi'+v_2/2, \tag{5.13}$$

then

$$fv=\partial\Phi'/\partial X, \quad (g/\theta_0)\theta=\partial\Phi'/\partial Z. \tag{5.14}$$

Again the Jacobian of the transformation is ζ/f and so it is mathematically valid as long as the vertical component of absolute vorticity is positive and finite.

Also,

$$rq=\zeta\partial\theta'/\partial Z. \tag{5.15}$$

As in Section 3, we measure potential vorticity by a pseudo Brunt-Väisälä frequency in an initial state of negligible v, i.e.,

$$N^2=(g/\theta_0)\partial\theta/\partial z_0=g(f\theta_0)^{-1}r(z_0)q. \tag{5.16}$$

Here z_0 is the vertical coordinate of a fluid particle in the initial state. Using $\mu=r(z_0)/r(Z)$, we find that

$$N^2=\mu(\partial^2\Phi'/\partial Z^2)[1-f^{-2}\partial^2\Phi'/\partial X^2]^{-1}, \tag{5.17}$$

is conserved following a fluid particle. On a "horizontal" boundary, since $w=0$ there, and using (5.19), we have

$$D=\partial/\partial T+s^2f^{-1}(Z-h)\partial/\partial X. \tag{5.18}$$

Here we have used $T=t$ as the time variable when X is our horizontal coordinate. Therefore, on a horizontal boundary the thermodynamic equation gives

$$[\partial/\partial T+s^2f^{-1}(Z-h)\partial/\partial X]\partial\Phi'/\partial Z = s^2f^{-1}\partial\Phi'/\partial X. \tag{5.19}$$

c. The Boussinesq, uniform N model

The motion of particles in the X, Z plane is the geostrophic x velocity plus the vertical velocity. Thus, in general, the value of N^2 as a function of position, at any time, is not known. However, we now restrict ourselves to the problem of Williams. We make the Boussinesq approximation $\mu\equiv 1$ and consider a fluid with N uniform initially, and hence for all time, bounded by horizontal boundaries at $z=0$, H. For convenience we choose $h=H/2$. From (5.17) and (5.19), the problem takes the closed form

$$\partial^2\Phi'/\partial X^2+(f^2/N^2)\partial^2\Phi'/\partial Z^2=f^2, \tag{5.20}$$

with

$$[\partial/\partial T+s^2f^{-1}(Z-H/2)\partial/\partial X]\partial\Phi'/\partial Z = s^2f^{-1}\partial\Phi'/\partial X \quad \text{on} \quad Z=0, H.$$

The transformation to physical space is given by

$$(x,z,t)=(X-f^{-2}\partial\Phi'/\partial X,\ Z,\ T). \tag{5.21}$$

The equations governing this nonlinear flow have thus been made linear. The nonlinearity now occurs only in the transformation to physical space. This is, however, easily accomplished graphically.

From the similarity of the approach to this model and the deformation model, it is clear that an attack should be made on a model including them both. This is done in the Appendix by transforming the equations of motion. There, for this model, it is shown that the x, z streamfunction such that

$$u=s^2f^{-1}(z-H/2)+\partial\psi^*/\partial z, \quad w=-\partial\psi^*/\partial x$$

satisfies

$$N^2\partial^2\psi^*/\partial X^2+f^2\partial^2\psi^*/\partial Z^2=-2s^2\partial v/\partial X. \tag{5.22}$$

On $Z=0$, H we demand $\psi^*=$constant. A closed streamline around an area of positive relative vorticity must have anticlockwise circulation around it. We note that the frontogenetic problem of determining v and θ, and the circulation problem have again separated. The streamfunction ψ^* need not be calculated to determine the solution of the frontogenetic problem. If the Boussinesq approximation had been made in the original equations and uniform N^2 assumed, the above equations would have been obtained directly.

Quasi-geostrophic theory when applied to this model gives the same equation and boundary condition (5.20) but with Φ', X, Z, T replaced by ϕ', x, z, t. As was true in the one-fluid deformation model, our balanced model must give the same values of v and θ' as quasi-geostrophic theory, but these values are predicted at $(X-v/f, Z)$. This distortion again implies $\zeta/f=2$, 0, while on quasi-geostrophic theory we have $\zeta/f=\infty$, $\frac{1}{2}$. Our solution to the baroclinic instability problem and the growth of the Eady wave is

$$\Phi' = N^2Z^2/2+\exp(s^2\sigma T/N)(a\cosh\beta\tilde{Z}\cos\beta\tilde{X} + b\sinh\beta\tilde{Z}\sin\beta\tilde{X}), \quad (5.23)$$

where

$$\left.\begin{array}{l} \tilde{Z}=(Z-H')/H', \quad \tilde{X}=fX/(NH'), \quad H'=H/2 \\ \sigma\dfrac{a}{b}=1-\beta\coth\beta, \quad \sigma\dfrac{b}{a}=\beta\tanh\beta-1 \end{array}\right\}.$$

For an infinitesimal wave, $X=x$ and the form is identical to the quasi-geostrophic Eady wave. The associated streamfunction is

$$\psi^* = \beta s^2 f^{-1}N^{-2}\exp(s^2\sigma T/N)[a(\tilde{Z}\sinh\beta\tilde{Z}-\tanh\beta\cosh\beta\tilde{Z}) \times\cos\beta\tilde{X}+b(\tilde{Z}\cosh\beta\tilde{Z}-\coth\beta\sinh\beta\tilde{Z}) \times\sin\beta\tilde{X}]. \quad (5.24)$$

d. Comparison with numerical integrations

To test our solution we compare it with the results of numerical integrations of this model for the most unstable Eady wave as described by Williams. The numerical solution at approximately the time at which our analytic theory suggests that the maximum absolute vorticity at the surface and the lid is $5f$ is shown in Fig. 10. Because of periodicity and the symmetry about $z=H/2$, we show only the lower half domain for one period. The corresponding analytic solution is exhibited in Fig. 11. The agreement between the two is extremely good. The largest gradients in the numerical solution are a little smaller than predicted. However, this may easily be explained by the round-off errors inherent in numerical integrations with a finite grid (20 grid points per wavelength), particularly when the differences in the values of quantities stored at neighboring grid points are so large.

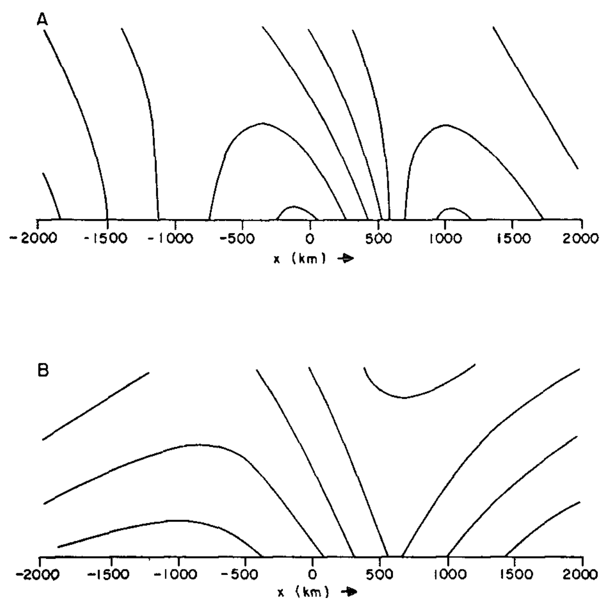

FIG. 10. The numerical solution for the finite-amplitude Eady wave: A, long-front velocity (contours every 15.2 m sec^{-1}); B, potential temperature (contours every 10.3K).

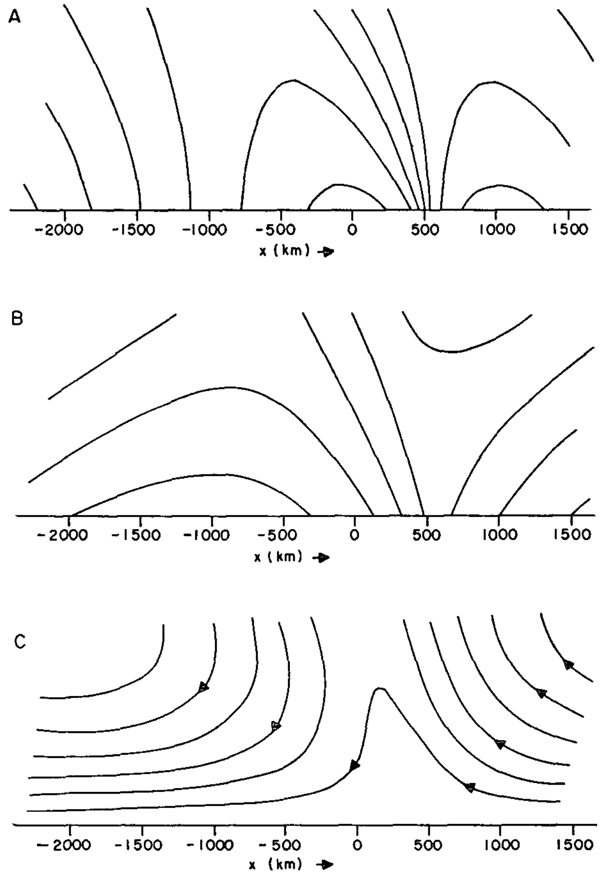

FIG. 11. The analytic solution for the finite-amplitude Eady wave: A and B as in Fig. 12; C, cross-front streamfunction.

For interest we exhibit in Fig. 13c the total cross-front streamfunction, $\psi^*+s^2(2f)^{-1}z(z-H')$. Since it is found that the position of maximum vorticity scarcely moves at this time, we may consider this as representing the flow relative to the front.

Our analysis suggests that the frontal model of Williams should have produced discontinuities in just over 5 days. This is consistent with the tendency to discontinuity which he found. This was halted only by lack of definition due to a finite grid. The "collapse" mechanism occurs at such a rate that infinite vorticity is predicted only 7 hr after the pictures shown.

Study of the consistency of the geostrophic balance approximation in this model shows that we must have

$$\zeta/f \ll (s^2 f^{-1} N^{-1} \sigma)^2 \approx 120.$$

Of much more concern is the behavior of the Richardson number. By the time $\zeta = 5f$, the minimum value at the surface front is 0.26. For ζ larger, from (2.31), we expect that $\mathrm{Ri} \approx f/\zeta$. Thus, before the balance approximation breaks down we again expect that mixing must be important. However, we may say that in this model exhibiting the horizontal shear effect, there is a tendency to form discontinuities in a finite time.

6. The formation of frontal discontinuities

We have produced models in which the initial temperature gradients in the x direction are produced by a large-scale deformation field and by a large-scale horizontal shearing motion. Associated with these temperature gradients, velocities in the y direction are formed in accordance with the thermal wind relation. If V is a characteristic velocity in the y direction and l a length scale in the x direction, when $V/(fl)$ is no longer negligible, the ageostrophic motion in x, z planes becomes important. It produces a distortion of the solution predicted by quasi-geostrophic theory. In particular, positive relative vorticity is increased and sloping frontal regions form. When the vorticity at a surface front is large compared with f, the ageostrophic motions dominate there and produce a tendency to form discontinuities in a finite time. It is clearly of interest to consider what approximations may be made in a strong frontal region, and to study the dynamics of this catastrophic tightening process.

In this section we study a general frontal region in which there are very large gradients in long-front velocity v and potential temperature θ. The dynamical model of this region was inspired by the frontal models exhibited in previous sections. However, it should be quite generally valid.

a. The equations

As in Section 2b, we take coordinate axes x in the cross-front direction pointing toward warmer air, y in the long-front direction, and z upward. Assuming that the curvature of the front may be neglected and making the assumption of geostrophic balance in the x direction, we have Eqs. (2.17)–(2.22) which may be rewritten as

$$Dv = -fu - \partial\phi/\partial y - v\partial u/\partial y, \qquad (6.1)$$

$$\partial(ru)/\partial x + \partial(rw)/\partial z = -\partial(rv)\partial y, \qquad (6.2)$$

$$D\theta = -v\partial\theta/\partial y, \qquad (6.3)$$

$$f\partial v/\partial z - (g/\theta_0)\partial\theta/\partial x = 0, \qquad (6.4)$$

where $D = \partial/\partial t + u\partial/\partial x + w\partial/\partial z$ is the derivative moving with the particle velocity in the planes $y = \text{constant}$.

Since gradients in the cross-front direction are so much larger than those in long-front direction we may, to a good approximation, neglect the y dependence of u, v, w and θ. We may consider the motion as that of y lines, and D as the derivative following these lines. Also, we may neglect the right-hand side of Eq. (6.2).

The final approximation is a rather novel one inspired by our frontal solutions. In these, and quite generally we expect, in the final stages of collapse to a discontinuity, the time scale is so small that the right-hand sides of Eqs. (6.1) and (6.3) may be neglected. They then state that v and θ are conserved moving with the y lines. For convenience, we restate the equations governing our model:

$$Dv = 0, \qquad (6.5)$$

$$D\theta = 0, \qquad (6.6)$$

$$\partial(ru)/\partial x + \partial(rw)/\partial z = 0, \qquad (6.7)$$

$$f\partial v/\partial z = (g/\theta_0)\partial\theta/\partial x, \qquad (6.8)$$

where

$$D = \partial/\partial t + u\partial/\partial x + w\partial/\partial z.$$

We may now define the "vorticity" $\boldsymbol{\zeta}' = (-\partial v/\partial z, 0, \partial v/\partial x)$. The vorticity equation is then

$$D(\boldsymbol{\zeta}'/r) = [(\boldsymbol{\zeta}'/r)\cdot\nabla]\mathbf{v}. \qquad (6.9)$$

The form taken by Ertel's potential vorticity is

$$q' = \boldsymbol{\zeta}'\cdot\nabla\theta/r. \qquad (6.10)$$

b. Analysis of a strong frontal region

1) When gradients are very large we expect that the earth's rotation will be negligible compared with the relative vorticity. Thus, $\boldsymbol{\zeta}'$ is a consistent approximation to $\boldsymbol{\zeta} = (-\partial v/\partial z, 0, f + \partial v/\partial x)$. Since v is independent of the long-front coordinate, the surfaces on which v is constant are perpendicular to a cross-front section. From the form of $\boldsymbol{\zeta}'$, the vortex lines must all lie in these v surfaces.

2) Ertel's potential vorticity q is conserved moving with a fluid particle and is thus bounded everywhere. In our limit q' is a consistent approximation to q. Thus, in our limit of indefinitely large gradients, we must

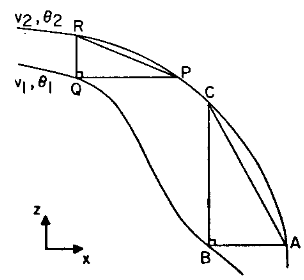

FIG. 12. Two neighboring v, θ surfaces.

have $\nabla\theta$ perpendicular to ζ'. Therefore, θ surfaces and v surfaces coincide.

3) Consider two neighboring v surfaces (Fig. 12) BQ on which $v=v_1$, $\theta=\theta_1$ and ACPR on which $v=v_2$, $\theta=\theta_2$. The balance condition [Eq. (6.8)] implies

$$\frac{v_2-v_1}{CB}=\frac{g}{f\theta_0}\frac{\theta_2-\theta_1}{AB},\quad \frac{v_2-v_1}{RQ}=\frac{g}{f\theta_0}\frac{\theta_2-\theta_1}{PQ}.$$

Then the slope of $AC=-CB/AB=-(f\theta_0/g)\times(v_2-v_1)/(\theta_2-\theta_1)$ and the slope of $PR=-RQ/PQ=-(f\theta_0/g)(v_2-v_1)/(\theta_2-\theta_1)$.

Therefore, the v surfaces are *planes* of slope

$$-f(\theta_0/g)\partial v/\partial\theta. \tag{6.11}$$

4) Since v and θ are conserved moving with y lines, they are conserved moving with these v planes. Thus, we may write $v=F(\theta)$ for some, as yet undetermined, function F. From (6.11), therefore, the slopes of the v planes are $-(f\theta_0/g)F'(\theta)$, and are thus constant in time.

5) Discontinuities may be formed only by the meeting of two v planes. Our model can predict the formation of discontinuities only on a boundary. To prove this, suppose on the contrary that one is to form at an interior point P (Fig. 13). A short time prior to this collapse, in some neighborhood of P, the v surfaces and θ surfaces are identical and plane. Contrary to hypothesis, discontinuities must occur at Q before they occur at P. Thus, the original statement is proved. This is consistent with our study in Section 2c of the Monge-Ampère equation satisfied by ϕ.

6) The v planes fan out from the boundary as, otherwise, discontinuities will have occurred at an interior point.

7) Our axes have been chosen so that $\partial\theta/\partial x$ is positive. Since this is necessarily positive for a stable situation, the slope of the θ planes and thus of v planes is negative. But $f\partial v/\partial z=(g/\theta_0)\partial\theta/\partial x$ is positive, and thus the relative vorticity $\partial v/\partial x$ is positive.

Fig. 14 is a drawing of our strong frontal region. The similarity with the strong frontal regions exhibited here and in H is clear.

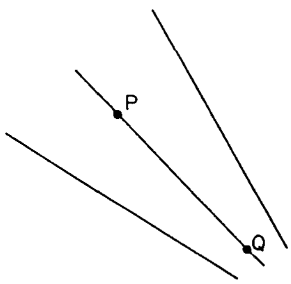

FIG. 13. v surfaces in the neighborhood of an interior point P.

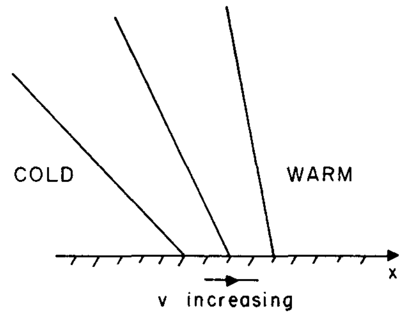

FIG. 14. Planes v = constant, θ = constant in a strong frontal region.

c. Analysis of the motion

The possible fluid motions in the region are those and only those that conserve the slopes of the v planes. These may be divided into two types: 1) motion in v planes, and 2) motion of v planes parallel to themselves. Clearly these motions do not change the slopes of v planes and, conversely, any motion that satisfies this criterion can be formed from them. Motion of type 2) must, by continuity, be associated with motion of type 1).

Mathematically, using a subscript v to denote a derivative holding v constant, we have

$$(\partial x/\partial t)_v=VF(v/V,t/T), \tag{6.12}$$

where F is a dimensionless function with characteristic velocity scale V and time scale T, and is arbitrary as far as our strong frontal region is concerned. It is evident from our solutions that it is determined from the interior region where the more general equations of motion are relevant. In particular, it has the time scale (T) of the interior. Therefore, in the time scale of collapse to a discontinuity, we may consider F as independent of time and rewrite Eq. (6.12) as

$$(\partial x/\partial t)_v=VF(v/V). \tag{6.13}$$

The v planes are decoupled, each moving with a constant velocity. If $F'<0$ anywhere, then v planes move toward one another with constant speed and the formation of a discontinuity is inevitable (see Fig. 15). The remainder of this section expresses this more exactly.

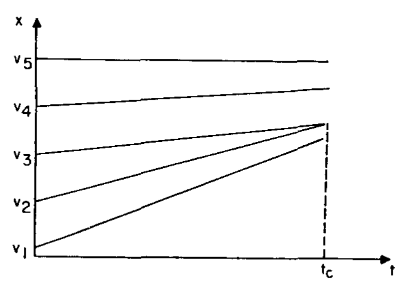

FIG. 15. The position (x) of v planes at the boundary as a function of time (t). Each moves with a constant velocity. Here discontinuities form at time t_c.

Since $w=0$ at the ground, there can be no type (i) motion there. The cross-front velocity must be $u=VF(v/V)$. Therefore,

$$\partial u/\partial x = F'\partial v/\partial x. \tag{6.14}$$

The convergence required to form large gradients implies that $F'<0$ in the region.

Since $(\partial x/\partial t)_v = -(\partial v/\partial t)(\partial v/\partial x)^{-1}$, (6.13) may be rewritten as

$$\partial v/\partial t + VF\partial v/\partial x = 0. \tag{6.15}$$

Differentiating with respect to x, we obtain the vertical vorticity equation

$$(\partial/\partial t + VF\partial/\partial x)\partial v/\partial x = -F'(\partial v/\partial x)^2,$$

or

$$(\partial/\partial t + VF\partial/\partial x)(\partial v/\partial x)^{-1} = F'. \tag{6.16}$$

We fix our attention on a fluid particle at the ground. For this particle, F' is constant. Integrating (6.16) from some initial time $t=0$, say, we have

$$\partial v/\partial x = (F')^{-1}[t-t_c(v)]^{-1}, \tag{6.17}$$

where

$$t_c(v) = -[F'(\partial v/\partial x)_0]^{-1} = -[(\partial u/\partial x)_0]^{-1}. \tag{6.18}$$

Therefore, discontinuities occur first at the ground at $v=v_m$ at which $-(\partial u/\partial x)_0$ takes its largest value t_m^{-1} and happens after a time t_m.

Within a certain range of the v_m plane, we may approximate F by

$$F(v/V) = A + Bv/V, \tag{6.19}$$

where A and B are nondimensional constants, with A corresponding to mere advection of the frontal region. The collapse to a discontinuity is controlled by the dimensionless, negative (since $F'<0$) number B, which is determined by the interior. Rewriting Eqs. (6.17) and (6.18) at the ground, we have

$$\partial v/\partial x = B^{-1}[t-t_c(v)]^{-1}, \tag{6.20}$$

where

$$t_c(v) = -[B(\partial v/\partial x)_0]^{-1}. \tag{6.21}$$

d. *The dimensionless number B*

It has been shown that the only effect of the interior on the "collapse" region is the rather subtle one of providing a negative dimensionless number B which controls the rate at which the collapse to a discontinuity proceeds. We now consider this number B.

From (6.14) we see that

$$B = (\partial u/\partial x)(\partial v/\partial x)^{-1} = -\frac{\text{deformation}}{\text{vertical vorticity}} \tag{6.22}$$

at the ground. It should be noted that since the ageostrophic deformation is dominant, a value for B may not be deduced from surface pressure charts. It can be estimated if surface wind data is available.

If the deformation model with zero potential vorticity it may be seen from (3.23) that $B=-2\alpha/f$. If we make the Boussinesq approximation, which should certainly be valid in a limited region near a rigid horizontal boundary, introduce a cross-front streamfunction, and use the geostrophic coordinate X, then, at the ground

$$\partial u/\partial x = \partial^2\psi^*/\partial x\partial z = (\partial^2\psi^*/\partial X\partial Z)\left(1+f^{-1}\frac{\alpha v}{\alpha x}\right).$$

Therefore,

$$B = f^1\partial^2\psi^*/\partial X\partial Z. \tag{6.23}$$

In frontal collapse in the general deformation model we see that $B=O(\alpha/f)$. For the collapse in the Eady wave, it may be verified from (5.26) that $B=-\sigma/f$ where σ is the growth rate of the wave. Thus, in our solutions, B is a measure of the ageostrophy of the interior motion. Using the values of parameters quoted earlier, we have $B=-0.2$, $B\approx O(0.1)$, $B\approx -0.09$. Quite generally, we expect B to be an order of magnitude smaller than unity.

e. *Discussion*

It was implicitly assumed in Section 6c that the collapse region is at a boundary z=constant. Now consider a general boundary to the fluid in the x, z plane. If large gradients are present near this boundary, then the above arguments show that there is a tendency for v and θ surfaces to be coincident and plane and to move together at a constant speed. There must be a tendency to form a discontinuity in a finite time unless the boundary is "flexible" enough to be sucked into the interior at a rate nullifying the moving together of the surfaces. The pressure at the boundary determines its z coordinate. Since the surface pressure on the earth is an integral quantity over the whole depth of the atmosphere and varies only within $\pm 5\%$, the flexibility of the earth's surface when viewed in our coordinates must be insufficient to halt the collapse process. Thus, we may expect a pressure trough at a surface front but not of sufficient magnitude to stop the tendency to form discontinuities there. However, as may be seen from the solutions in H, the tropopause when considered as a boundary for the troposphere does have this flexibility. It descends at such a rapid rate that there is no tendency to form discontinuities there. This is shown schematically in Fig. 16. In descending, it takes the form of an upper air front.

It is clear that the model of a strong frontal region introduced in this section depends on gradients being large enough that the potential vorticity, $q=f\partial\theta/\partial z_0$, may be neglected compared with the term $\zeta\partial\theta/\partial z$. This is never true in the stratospheric region of the solutions of the two-region model, and we do not expect our model to be applicable there. The decoupling of v planes and their motion with constant speed is dependent on the ability of particles to move up v, θ planes without

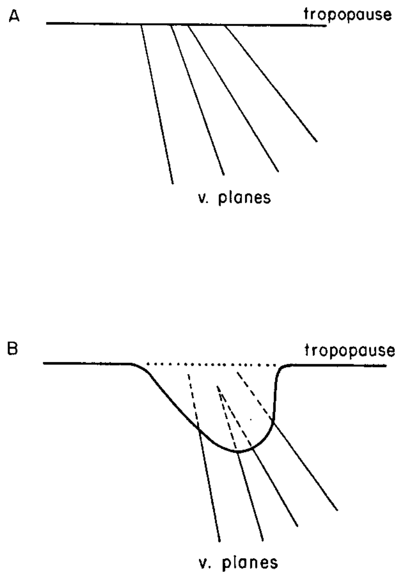

FIG. 16. Schematic description of the "non-collapse" process under the tropopause: A, large gradients form; B, collapse is prevented by the subsidence of the tropopause.

resistance from buoyancy forces. The similarity of the solution of our zero potential vorticity model to the far more realistic models introduced later is a clear indication that it does, indeed, include the essential mechanisms relevant in the collapse tendency of surface fronts.

f. The breakdown of our models

Although the original frontal model was a surface of discontinuity, discontinuities do not form in the atmosphere. We have made an assumption of cross-front geostrophic balance in all our work. It is certainly valid when the motion is quasi-geostrophic and the integrations of Williams (1967) suggest that it is valid in his model until the vorticity becomes large. We now investigate the approximation in our frontal collapse model.

Taking the boundary as $z=0$ and making the Boussinesq approximation, the cross-front streamfunction is

$$\psi^* = zVF(v/V) = AzV + BzV. \tag{6.24}$$

This gives

$$u = AV + Bv + Bz\partial v/\partial z, \tag{6.25}$$

$$w = -Bz\partial v/\partial x. \tag{6.26}$$

The motion consists of motion of v planes $(AV+Bv, 0, 0)$ and motion in v planes $(Bz\partial v/\partial z, v, -Bz\partial v/\partial x)$. From Eqs. (6.25) and (6.26), the balance approximation is consistent if and only if

$$f^{-1}\partial v/\partial x \ll B^{-2}. \tag{6.27}$$

Recalling the order of magnitude of B, we see that this is a very weak condition, typically demanding $\zeta \ll 100f$.

The real breakdown of our models is that when gradients become large, we must have [Eq. (2.31)] $\mathrm{Ri} \approx f/\zeta$. Before $\zeta = 10f$, $\mathrm{Ri} \approx 0.1$, Kelvin-Helmholtz instability must be expected, and neglected mixing effects must be important.

The effect of mixing on our models is unclear. It will tend to stop gradients becoming larger at the surface front. Away from the surface, however, v planes may continue to move together. In this way a front with large gradients over a more substantial part of the troposphere could be formed.

7. Conclusion

In this paper we distinguish between large-scale geostrophic processes which intensify horizontal temperature gradients, and smaller scale ageostrophic motions embedded in the baroclinic flow which lead to the rapid formation of a near discontinuity. Two such geostrophic mechanisms are isolated: the classical horizontal deformation field, and the growing baroclinic wave investigated by Williams. In each case, when the relative vorticity predicted by the quasi-geostrophic theory approaches the value of the Coriolis parameter, small-scale ageostrophic circulations which were hitherto negligible become dominant and a near discontinuity forms abruptly on a rigid boundary such as the earth's surface. Imposed in these models is uniformity of conditions along the incipient front. A scale analysis suggests that cross-front geostrophic balance is a good first approximation throughout this process and the consistency of this assumption is verified *a posteriori*. The breakdown of the analysis in the final stages of this collapse to a near discontinuity occurs first because the Richardson number falls to such low values that small-scale instability and a breakdown to clear air turbulence are to be expected. If this instability did not occur, the geostrophic balance would fail locally at a later stage.

This study confirms that the potential for forming sharp fronts is implicit in the inviscid, adiabatic primitive equations of motion alone. This conclusion had previously been suggested by the numerical integrations of Edelmann and Williams. An examination of the dominant terms in the equations of motion during the final stages of the collapse process reveals that, locally, surfaces of constant potential temperature and constant long-front velocity are plane and coincident, and these planes converge at a constant rate, moving without change of slope. This process which implies the formation of a discontinuity in a finite time is quite general and proceeds inexorably once the relative vorticity has become large. From our work it may be inferred that sharp surface fronts will form whenever quasi-geostrophic theory predicts a band of relative vorticity at the earth's surface of magnitude comparable to the Coriolis parameter.

A sequence of models of increasing complexity yield realistic cross sections of surface fronts. However, the simplest model in which the potential vorticity vanishes shows qualitatively all the significant features to a remarkable degree. The effects of the Boussinesq approximation and imposing a "rigid" lid are examined and found to be small. The extent to which these models reproduce the observed features of fronts in the real atmosphere suggests that latent heat release and surface friction are secondary to the process of front formation, although they certainly modify substantially the details. Rather crude estimates of these effects in the models support this idea. Latent heat release enhances frontogenesis whereas surface friction is frontolytic. The inviscid, adiabatic dynamics makes no distinction between cold and warm fronts and, in this respect, the picture presented is incomplete. In particular, were extensive cumulonimbus convection to set in, our models might have little relevance.

A deformation field intensifying horizontal temperature gradients in a system with a large potential vorticity contrast between the troposphere and the stratosphere induces upper tropospheric fronts. The dynamical balance is very similar to that described above for surface fronts except that the tropopause does not behave quite like a rigid boundary. Our models exhibit descent of a tongue of stratospheric air through a substantial distance. These solutions closely resemble the cross sections published by Reed and Sanders in their study from the synoptic data of an intense upper air front. However, the Richardson number at the base of the tongue falls below unity after a descent of 118 mb, which is not as far as the ultimate penetration of stratospheric air shown in many studies. We infer that clear air turbulence is likely to be of importance in the later stages of the process. It should be noted that the development in the upper troposphere appears to be rather insensitive to the details of the surface flow pattern.

The vertical coordinate used in this study is a certain function of the pressure rather than the pressure itself. This has the advantage of simplifying the thermal wind equation and exhibiting clearly the relation between the Boussinesq approximation and the fully compressible equations.

A transformation of coordinates proves fruitful in which the cross-front position of a particle is described by the position it would have had if it had always moved with the local geostrophic velocity. The significance of this geostrophic coordinate is suggested by Kelvin's circulation theorem. The constancy of potential temperature and potential vorticity following a material particle taken in conjunction with the thermal wind relation then provide a description of the instantaneous geopotential field which satisfied an elliptic partial differential equation (3.34). By a description in terms of conserved quantities we thus produce a great mathematical and conceptual simplification. The system proceeds through a sequence of states, each of which can be considered separately from the intermediate history and can be linked directly to the initial conditions. This illustrates the limitations as well as the advantages of the method. After the solution for the geopotential, the cross-front circulation may be found in a diagnostic manner.

The finite-amplitude baroclinic instability model, which Williams investigated numerically, is found to be capable of exact analytic solution, subject to cross-front geostrophic balance. This model assumes the Boussinesq approximation, uniform Brunt-Väisälä frequency, a uniform meridional temperature gradient, and no lateral boundaries. Under such conditions there is an infinite source of available potential energy which feeds the unstable baroclinic disturbance within which a sharp front develops. However, this frontogenesis occurs only after the wave has grown to unreasonably large amplitude. For this model, the balanced solution is formally identical to that of the quasi-geostrophic equations, but the interpretation of the horizontal independent variable is different. Thus, our theory only predicts a distortion of the quasi-geostrophic solution, but this distortion is vital in the description of the frontogenesis. In particular, where the quasi-geostrophic theory predicts the relative vorticity is equal to f, the balanced theory predicts that it has become infinite. A similar correspondence also occurs in the deformation model when the potential vorticity is uniform and the Boussinesq approximation is made. However, this exact correspondence does not appear to be general.

Acknowledgments. One of us (BJH) was supported for two years at the Department of Applied Mathematics and Theoretical Physics in the University of Cambridge by a research studentship given by the Natural Environment Research Council. Following this, both authors were supported at The Johns Hopkins University by the National Science Foundation under Grant GA-16603.

APPENDIX

A General Model

a. *Transformations of the equations*

In this appendix we study the equations for a quite general model which includes the horizontal deformation and horizontal shear models. We use the general equations of motion (2.6)–(2.9) with a diabatic heating term. The basis of the study is an approximation of balance in the x direction and a transformation of variables.

Without loss of generality, we may set

$$\left.\begin{aligned} u&=-\alpha x+u' \\ v&=\alpha y+v' \\ w&=w' \\ \phi&=f\alpha xy-(\alpha^2+d\alpha/dt)y^2/2 \\ &\quad -(\alpha^2-d\alpha/dt)x^2/2+\phi' \\ \theta&=\theta'=(\theta_0/g)\partial\phi'/\partial z \end{aligned}\right\}, \tag{A1}$$

where $\alpha=\alpha(t)$, and all primed variables are, in general, functions of x, y, z, t. Then the equations may be written as

$$Du'/Dt-\alpha u'-fv'+\partial\phi'/\partial x=0, \tag{A2}$$

$$Dv'/Dt+\alpha v'+fu'+\partial\phi'/\partial y=0, \tag{A3}$$

$$\partial(ru')/\partial x+\partial(rv')/\partial v+\partial(rw')/\partial z=0, \tag{A4}$$

$$D\theta'/Dt=E. \tag{A5}$$

Scale analysis (as in Section 2b) and observation suggest that the first two terms in (A2) may be neglected even when there are large frontal gradients in the x direction. This is the only approximation that we make. We note that if we now set

$$\phi''=f\alpha xy-(\alpha^2+d\alpha/dt)y^2/2+\phi'=\phi+(\alpha^2-d\alpha/dt)x^2/2,$$

we obtain the equations with "geostrophic balance in the x direction" [Eqs. (2.17)–(2.22)] except that ϕ'' differs from the geopotential by a negligible correction term.

We define

$$u_g'=-f^{-1}\partial\phi'/\partial y,\quad v_g'=f^{-1}\partial\phi'/\partial x,\quad u_{ag}'=u'-u_g'.$$

Then (A2)–(A4) give

$$\left.\begin{aligned} Dv_g'/Dt+\alpha v_g'+fu_{ag}'&=0 \\ \partial(ru_{ag}')/\partial x+\partial(rw')/\partial z&=0 \end{aligned}\right\}. \tag{A6}$$

The latter equation implies that we may define a pseudo streamfunction ψ such that

$$ru_{ag}'=\partial\psi/\partial z,\quad rw'=-\partial\psi/\partial x. \tag{A7}$$

We now use as independent variables

$$(X,Y,Z,T)=[x+v_g'/(f,y,z,t)]. \tag{A8}$$

Formally, we have

$$\partial/\partial x=(\zeta/f)\partial/\partial X, \tag{A9}$$

and so

$$\zeta=f[1-f^{-1}\partial v_g'/\partial X]^{-1}, \tag{A10}$$

$$\frac{\partial}{\partial y}=\frac{1}{f}\frac{\partial v_g'}{\partial y}\frac{\partial}{\partial X}+\frac{\partial}{\partial Y}=-\frac{1}{f}\frac{\zeta}{f}\frac{\partial u_g'}{\partial X}\frac{\partial}{\partial X}+\frac{\partial}{\partial Y}, \tag{A11}$$

$$\frac{\partial}{\partial z}=\frac{1}{f}\frac{\partial v_g'}{\partial z}\frac{\partial}{\partial X}+\frac{\partial}{\partial Z}=\frac{g}{f^2\theta_0}\frac{\zeta}{f}\frac{\partial\theta'}{\partial X}\frac{\partial}{\partial X}+\frac{\partial}{\partial Z}. \tag{A12}$$

Then

$$\partial u_g'/\partial x=-\partial v_g'/\partial y\rightarrow\partial u_g'/\partial X=-\partial v_g'/\partial Y, \tag{A13}$$

$$f\partial v_g'/\partial z=(g/\theta_0)\partial\theta'/\partial x\rightarrow f\partial v_g'/\partial z=(g/\theta_0)\partial\theta'/\partial X, \tag{A14}$$

$$f\partial u_g'/\partial z=-(g/\theta_0)\partial\theta'/\partial y\rightarrow f\partial ug'/\partial Z=-(g/\theta_0)\partial\theta'/\partial Y. \tag{A15}$$

Hence the transformation preserves the geostrophic relations. This may be restated: There exists a function Φ such that

$$fu_g'=-\partial\Phi/\partial Y,\quad fv_g'=\partial\Phi/\partial x,\quad (g/\theta_0)\theta'=\partial\Phi/\partial Z. \tag{A16}$$

It may be verified that $\Phi=\phi'+v_g'^2/2$.

Using (A6), we then have

$$DX/Dt=u+f^{-1}Dv_g'/Dt=-\alpha X+u_g'. \tag{A17}$$

As before, X may be termed a geostrophic coordinate since if a fluid particle moves with $u_{ag}'=0$, its x coordinate is X. Using (A7) and transforming, the equations of motion may be written as

$$r(\mathfrak{D}+\alpha)v_g'+f\partial\psi/\partial Z=0, \tag{A18}$$

$$\mathfrak{D}\theta'-f^{-1}q\partial\psi/\partial X=E, \tag{A19}$$

where

$$\mathfrak{D}=\partial/\partial T+(-\alpha X+u_g')\partial/\partial X+(\alpha Y+v_g')\partial/\partial Y, \tag{A20}$$

$$rq=\zeta\partial\theta'/\partial Z. \tag{A21}$$

From (A18) we obtain the vorticity equation

$$r\mathfrak{D}\partial v'/\partial X+f\partial^2\psi/\partial X\partial Z=0, \tag{A22}$$

and from (A19)

$$\mathfrak{D}\partial\theta'/\partial Z-(\partial/\partial Z)(qf^{-1}\partial\psi/\partial X)=\partial E/\partial Z. \tag{A23}$$

From (A10), (A21), (A22), and (A23) it is easily found that

$$\left(\mathfrak{D}-\frac{1}{r}\frac{\zeta}{f}\frac{\partial\psi}{\partial X}\frac{\partial}{\partial Z}\right)q=\frac{\zeta}{r}\frac{\partial E}{\partial Z}. \tag{A24}$$

But

$$q=\frac{1}{r}\frac{\zeta}{f}\frac{\partial(fX,\theta')}{\partial(X,Z)}=\frac{1}{r}\frac{\partial(fX,\theta')}{\partial(x,z)},$$

$$=\frac{1}{r}\left[\left(f+\frac{\partial v_g'}{\partial x}\right)\frac{\partial\theta'}{\partial z}-\frac{\partial v_g'}{\partial z}\frac{\partial\theta'}{\partial x}\right], \tag{A24}$$

and $rw=-(\zeta/f)\partial\psi/\partial X$. Therefore, (A24) is Ertel's potential vorticity equation.

To investigate the vertical circulation we subtract $(g/\theta_0)\partial/\partial X$ of (A19) from $f\partial/\partial Z$ of (A18) to give

$$f^2\frac{\partial}{\partial Z}\left(\frac{1}{r}\frac{\partial\psi}{\partial Z}\right)+\frac{g}{f\theta_0}\frac{\partial}{\partial X}\left(q\frac{\partial\psi}{\partial X}\right)=-Q, \tag{A25}$$

where

$$\left.\begin{aligned} Q&=(g/\theta_0)\partial E/\partial X\\ &\quad+2f\partial(v_g', -\alpha X+u_g')/\partial(X,Z)\\ &=(g/\theta_0)\partial E/\partial X\\ &\quad+2f\partial(\alpha y+v_g', -\alpha x+u_g')/\partial(X,Z) \end{aligned}\right\}. \quad \text{(A26)}$$

This is equivalent to the circulation equation of Eliassen (1962). The equation predicts anticlockwise circulation (viewed form the negative y axis) about a streamline closed around an area over which $\int\int QdXdZ$ is positive.

We now consider the case of zero diabatic heating. Using (A19) and (A24), it is seen that conservation of potential temperature and potential vorticity give

$$(\partial q/\partial Z)^{-1}\mathfrak{D}q=(\partial\theta'/\partial Z)^{-1}\mathfrak{D}\theta'. \quad \text{(A27)}$$

From (A21), using (A16),

$$f^{-2}\partial^2\Phi/\partial X^2+[f\theta_0/(grq)]\partial^2\Phi/\partial Z^2=1. \quad \text{(A28)}$$

On horizontal boundaries we must have

$$\mathfrak{D}\theta'=0. \quad \text{(A29)}$$

In these equations,

$$\mathfrak{D}=\partial/\partial T+(-\alpha X+u_g')\partial/\partial X+(\alpha Y+v_g')\partial/\partial Y \quad \text{(A30)}$$

and

$$fu_g'=-\partial\Phi/\partial Y, \quad fv_g'=\partial\Phi/\partial X,$$
$$(g/\theta_0)\theta'=\partial\Phi/\partial Z. \quad \text{(A31)}$$

The transformation to physical space is $(x,y,z,t)=(X-f^{-2}\partial\Phi/\partial X,Y,Z,T)$. Thus, the frontogenetic problem for Φ and hence v_g' and θ' has split off from the problem for the circulation.

b. The deformation model

We look for a solution with α non-zero and Φ independent of Y. Then (A27) may be integrated to give

$$q(X,\theta',T)=q\left\{X\exp\left[\int_0^T\alpha(t)dt\right],\theta',0\right\}. \quad \text{(A32)}$$

The boundary condition (A29) also integrates to give

$$\theta'(X,bdry,T)=\theta'\left\{X\exp\left[\int_0^T\alpha(t)dt\right],bdry,0\right\}. \quad \text{(A33)}$$

Thus, with (A28) and (A31), we have the equations derived in Section 3.

In this model, the circulation equation is (A25) with

$$Q=2\alpha f\partial v_g'/\partial Z=2\alpha(g/\theta_0)\partial\theta'/\partial X. \quad \text{(A34)}$$

Thus, we must have anticlockwise flow around closed streamlines inside which $\int\int(\partial\theta'/\partial X)dXdZ$ is positive.

In particular, we expect a tendency for a thermodynamically direct circulation to occur, i.e., warm air rising, cold air subsiding.

c. The Boussinesq approximation and $\partial\theta/\partial z$ uniform initially

Suppose that in an initial state of zero x and z gradients in v, $\partial\theta/\partial z$ is uniform. If a particle is initially at z_0, then

$$\partial\theta/\partial z_0=f^{-1}r(z_0)q,$$

and conservation of q implies that $q^*=r(z_0)q$ remains uniform. Supposing that particles do not move a vertical distance comparable with the scale height, we make the Boussinesq type approximation, $r(z_0)/r(z)=1$, and set $N^2=(g/\theta_0)(q^*/f)$. Then (A28) becomes

$$f^{-2}\partial^2\Phi/\partial X+N^{-2}\partial^2\Phi/\partial Z^2=1. \quad \text{(A35)}$$

On horizontal boundaries,

$$[\partial/\partial T-(\alpha X+f^{-1}\partial\Phi/\partial Y)\partial/\partial X$$
$$+(\alpha Y+f^{-1}\partial\Phi/\partial X)\partial/\partial Y]\partial\Phi/\partial Z=0. \quad \text{(A36)}$$

The mathematical form of this system is the same as would be obtained on quasi-geostrophic theory provided $|\partial u/\partial y|\ll f$. This theory predicts only a distortion of the quasi-geostrophic solution for v and θ.

One example of this model is the one-layer deformation model in Section 3. There, $\alpha\neq 0$, $\Phi=\Phi(X,Z,T)$, and there are horizontal boundaries at $z=0$ and H. Horizontal gradients in Φ are zero everywhere initially and at infinity for all time.

Another example is the shear model of Section 4. Here $\alpha=0$, $\Phi=-s^2YZ+\Phi'(X,Z,T)$, and flow is between horizontal boundaries at $Z=0$, H. Under the Boussinesq approximation, $\psi^*=\psi/r$ is the usual streamfunction for the x, z circulation. Using the same approximation in the circulation equation we have

$$f^2\partial^2\psi^*/\partial Z^2+N^2\partial^2\psi^*/\partial X^2=-2s^2\partial v_g'/\partial X. \quad \text{(A37)}$$

Thus, we expect anticlockwise circulation where the vorticity is positive.

REFERENCES

Arakawa, A., 1962: Non-geostrophic effects in the baroclinic prognostic equations. *Proc. Intern. Symp. Numerical Weather Prediction*, Tokyo, 161–175.

Bergeron, T., 1928: Über die dreidimensional verknüpfende Wettranalyse I. *Geofys. Publikasjoner*, **5**, No. 6, 1–111.

——, 1937: On the physics of fronts. *Bull. Amer. Meteor. Soc.*, **18**, 265–275.

Bjerknes, J., and E. Palmèn, 1937: Investigations of selected European cyclones by means of serial ascents. *Geofys. Publikasjoner*, **12**, No. 2, 1–62.

Danielsen, E. F., 1968: Stratospheric-tropospheric exchange based on radio-activity, ozone and potential vorticity. *J. Atmos. Sci.*, **25**, 502–518.

Edelmann, W., 1963: On the behaviour of disturbances in a baroclinic channel. Summary Rept. No. 2, Research in

Objective Weather Forecasting, Part F, Contract No. AF61(052)-373, Deutscher Wetterdienst, Offenbach, 35 pp.

Eliassen, A., 1959: On the formation of fronts in the atmosphere. *The Atmosphere and the Sea in Motion*, New York, Rockefeller Institute Press, 277–287.

——, 1962: On the vertical circulation in frontal zones. *Geofys. Publikasjoner*, **24**, No. 4, 147–160.

——, and E. Kleinschmidt, 1957: Dynamic meteorology. *Handbuch der Physik*, Vol. 58, Berlin, Springer-Verlag, 1–154.

Faller, A. J., 1956: A demonstration of fronts and frontal waves in atmospheric models. *J. Meteor.*, **13**, 1–4.

Fultz, D., 1952: On the possibility of experimental models of the polarfront wave. *J. Meteor.*, **9**, 379–384.

Heinz, E., 1961: Interior estimates for solutions of elliptic Monge-Ampère equations. *Proc. Symp. Pure Mathematics, Vol. IV, Partial Differential Equations*, Providence, R. I., Amer. Math. Soc., 149–155.

Hoskins, B. J., 1970: Atmospheric frontogenesis. Ph.D. thesis, University of Cambridge.

——, 1971: Atmospheric frontogenesis: Some solutions. *Quart. J. Roy. Meteor. Soc.*, **97**, 139–153.

Manabe, S., J. Smagorinsky, J. L. Holloway and H. M. Stone, 1970: Simulated climatology of a general circulation model with a hydrologic cycle: III. Effects of increased horizontal computational resolution. *Mon. Wea. Rev.*, **98**, 175–212.

Namias, J., and P. F. Clapp, 1949: Confluence theory of the high tropospheric jet stream. *J. Meteor.*, **6**, 330–336.

Newell, R. E., 1963: Transfer through the tropopause and within the stratosphere. *Quart. J. Roy. Meteor. Soc.*, **89**, 167–204.

Pedlosky, J., 1964: The stability of currents in the atmosphere and ocean: Part I. *J. Atmos. Sci.*, **21**, 201–219.

Reed, R. J., 1955: A study of a characteristic type of upper-level frontogenesis. *J. Meteor.*, **12**, 226–237.

——, and E. F. Danielsen, 1959: Fronts in the vicinity of the tropopause. *Arch. Meteor. Geophys. Bioklim.*, **A11**, 1–17.

——, and F. Sanders, 1953: An investigation of the development of a mid-tropospheric frontal zone and its associated vorticity field. *J. Meteor.*, **10**, 338–349.

Sanders, F., 1955: Investigation of the structure and dynamics of an intense surface frontal zone. *J. Meteor.*, **12**, 542–552.

Sawyer, J. S., 1956: The vertical circulation at meteorological fronts and its relation to frontogenesis. *Proc. Roy. Soc. London*, **A234**, 346–362.

Stone, P. H., 1966: Frontogenesis by horizontal wind deformation fields. *J. Atmos. Sci.*, **23**, 455–465.

University of Chicago, 1947: On the general circulation of the atmosphere in middle latitudes. *Bull. Amer. Meteor. Soc.*, **28**, 255–280.

Williams, R. T., 1967: Atmospheric frontogenesis: A numerical experiment. *J. Atmos. Sci.*, **24**, 627–641.

——, 1968: A note on quasi-geostrophic frontogenesis. *J. Atmos. Sci.*, **25**, 1157–1159.

——, and J. Plotkin, 1968: Quasi-geostrophic frontogenesis. *J. Atmos. Sci.*, **25**, 201–206.